**Westinghouse**　　Energy Systems
**Electric Corporation**

Box 355
Pittsburgh Pennsylvania 15230-0355

NTD-NRC-96-4622
DCP/NRC0447
Docket No.: STN-52-003

January 12, 1996

Document Control Desk
U.S. Nuclear Regulatory Commission
Washington, D.C. 20555

ATTENTION:　　T. R. QUAY

SUBJECT:　　WESTINGHOUSE RESPONSES TO NRC REQUESTS FOR ADDITIONAL
　　　　　　　INFORMATION ON THE AP600
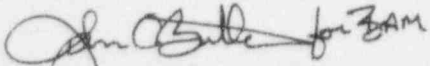
Dear Mr. Quay:

Enclosed are three copies of the Westinghouse responses to NRC requests for additional information
on the AP600 Design Certification Test Program. Topics discussed in this transmittal include the
NOTRUMP compute code, LOFTRAN computer code and the CMT Final Data Report. A listing of
the NRC requests for additional information responded to in this letter is contained in Attachment A.
These responses are also provided as electronic files in WordPerfect 5.1 format with Mr. Kenyon's
copy.

Correspondence with respect to this transmittal should be addressed to Brian A. McIntyre, Manager of
Advanced Plant Safety and Licensing, Westinghouse Electric Corporation, P.O. Box 355, Pittsburgh,
Pennsylvania, 15230-0355.

2652A

E004
1/1

Please contact Brian A. McIntyre on (412) 374-4334 if you have any questions concerning this transmittal.


Brian A. McIntyre, Manager
Advanced Plant Safety and Licensing

/nja

Attachments
Enclosures

cc:   T. Kenyon, NRC (w/o enclosures/attachments)
      W. Huffman, NRC (1E)
      R. C. Jones, NRC (w/o enclosures/attachments)
      G. D. McPherson, NRC (w/o enclosures/attachments)
      F. Eltawila, NRC (w/o enclosures/attachments)
      R. Landry, NRC (1E)
      L. Lois, NRC (1E)
      A. Levin, NRC (1E)
      P. Boehnert, ACRS (4E)
      N. J. Liparulo, Westinghouse (w/o enclosures/attachments)

# ATTACHMENT A

RAI's addressed in the January 12, 1996 submittal:

LOFTRAN      440.282
                 440.286
                 440.291
                 440.305

CMT FDR     440.361
                 440.362

NOTRUMP    440.440
                 440.464
                 440.493
                 440.509

AP600

**Question 440.282**

Why is the CMT fluid put into the cold legs in LOFTRAN when the plant geometry dictates that it be put into the vessel? Has this approximation been verified against experimental data or other code modelling for the AP600?

**Response:**

The CMT injection line is coupled to the RCS using coding already in place in the original LOFTRAN code for the simulation of the safety injection (SI) system. This method has the advantage of minimizing the modification of the original LOFTRAN code.

This approximation does not affect the CMT flow calculation because the local pressure in the downcomer is used in the model for calculating CMT flow rate (see response to RAI 440.291). However, the transfer of the highly borated CMT water to the core is delayed by the transit time of water in the cold leg between the simulated injection point and direct vessel injection (DVI) point. This effect is conservative with respect to safety analysis of design basis events, particularly the steamline break core response event which relies on boration from the CMTs for shutdown.

**SSAR Revision: NONE**
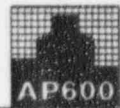
Question 440.286

Re: WCAP-14234 (LOFTRAN CAD)

Section 3.1, page 3-1. Please provide a stability analysis of the CMT model that determines the time step bounds for the CMT. Also, please show how the stability of the model is affected by any explicit connection to the RCS.

Response:

### Stability Analysis of the CMT Model

The time step influence on the CMT model response was analyzed in Reference 440.286-1. The CMT Test C064506 (Matrix Test 506) was selected and the conclusion was that the response is independent of the CMT time step for time steps in the range of one second or less.

The analysis contained in Reference 440.286-1 is expanded and results from two additional runs are presented in this RAI response, in order to identify the range of time steps acceptable for the CMT module for Matrix Test 506. Table 440.286-1 provides the time step used for each run. Runs 3 and 4 were presented in Reference 440.286-1.

Figures 440.286-1 through 440.286-12 provide the key parameters for each run. Run 3 is selected as the base case and the other runs are compared to this base case.

The comparison of Run 3 with Runs 2 and 4 (Figures 440.286-5 to 440.286-12) shows that the CMT module response is independent of the CMT time step for time steps less than 2.5 seconds. The plots are superimposed and it is almost impossible to differentiate the results. This demonstrates that the LOFTRAN CMT numerics are stable when used within the acceptable time step range. This is always the case for the AP600 SSAR analyses performed using LOFTRAN-AP or LOFTTR2-AP.

Figure 440.286-1 shows that the CMT model is not stable with a time step of 5 seconds, especially between time zero and 1000 seconds. The injection flow rate oscillates around the solution of run 3. The flow oscillations have a small impact on the other parameters (Figure 440.286-2, 440.286-3, and 440.286-4). This proves that the limiting equation with respect to time step stability is the momentum equation of the lines connecting the RCS and CMTs which is solved explicitly (see response to RAI 440.285).

### Explicit Connection to the RCS

Due to the design, the CMT injection flow is single phase in transients analyzed with LOFTRAN and is almost independent of the RCS absolute pressure. Since the CMTs operate after the RCPs trip, the pressure difference between the CMT balance line inlet and the CMT injection line outlet is essentially the buoyancy of the water in the RCS downcomer, which does not vary significantly over time.

The coupling between the CMT and the RCS was verified during the SPES-2 SGTR simulations. The results of the SPES-2 Matrix Test 10 simulations (Reference 440.286-1 - Test 10 Run 6 and 7) are not affected by a variation of the LOFTRAN main time step by a factor of two. The detail of the connection between the CMTs and the RCS is provided in the response to RAI 440.291.

---

Westinghouse

**AP600**

References

440.286-1    WCAP-14307, "AP600 LOFTRAN-AP and LOFTTR2-AP Final Verification and Validation Report," June 1995

SSAR Revision: NONE

**Westinghouse**

| TABLE 440.286-1 CMT TEST C064506 - TIME STEP SENSITIVITY STUDY | | |
|---|---|---|
| **Run number** | **DT** | |
| | **Time 0 to 10 sec** | **Time 10 to 3000 sec** |
| Run 1 | 1 | 5 |
| Run 2 | 0.5 | 2.5 |
| Run 3 | 0.2 | 1 |
| Run 4 | 0.05 | 0.25 |

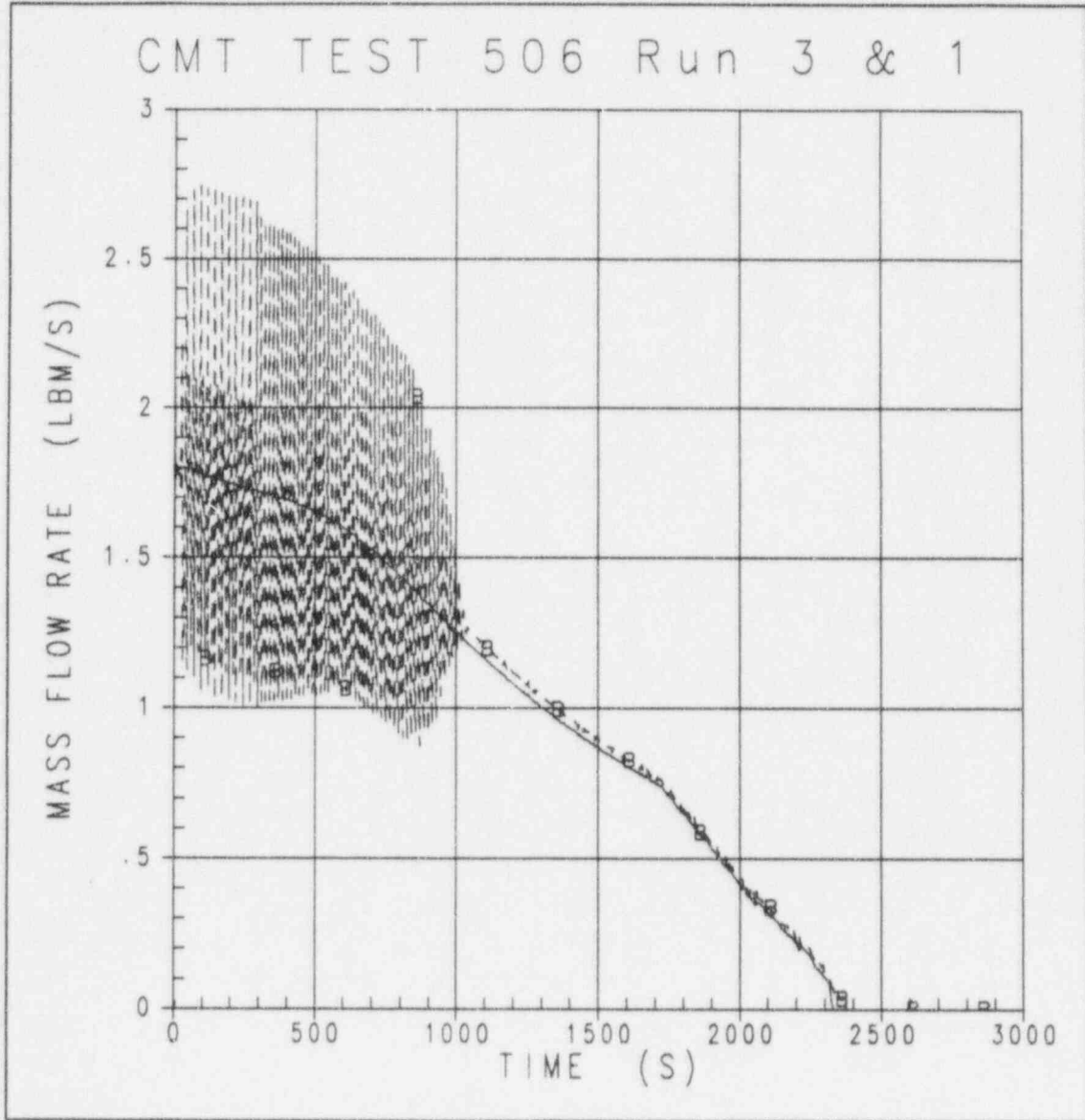**Figure 440.286-1**      C064506 Test, Injection Line Flow Rate

_____  LOFTRANCMT Calculation - Run 3
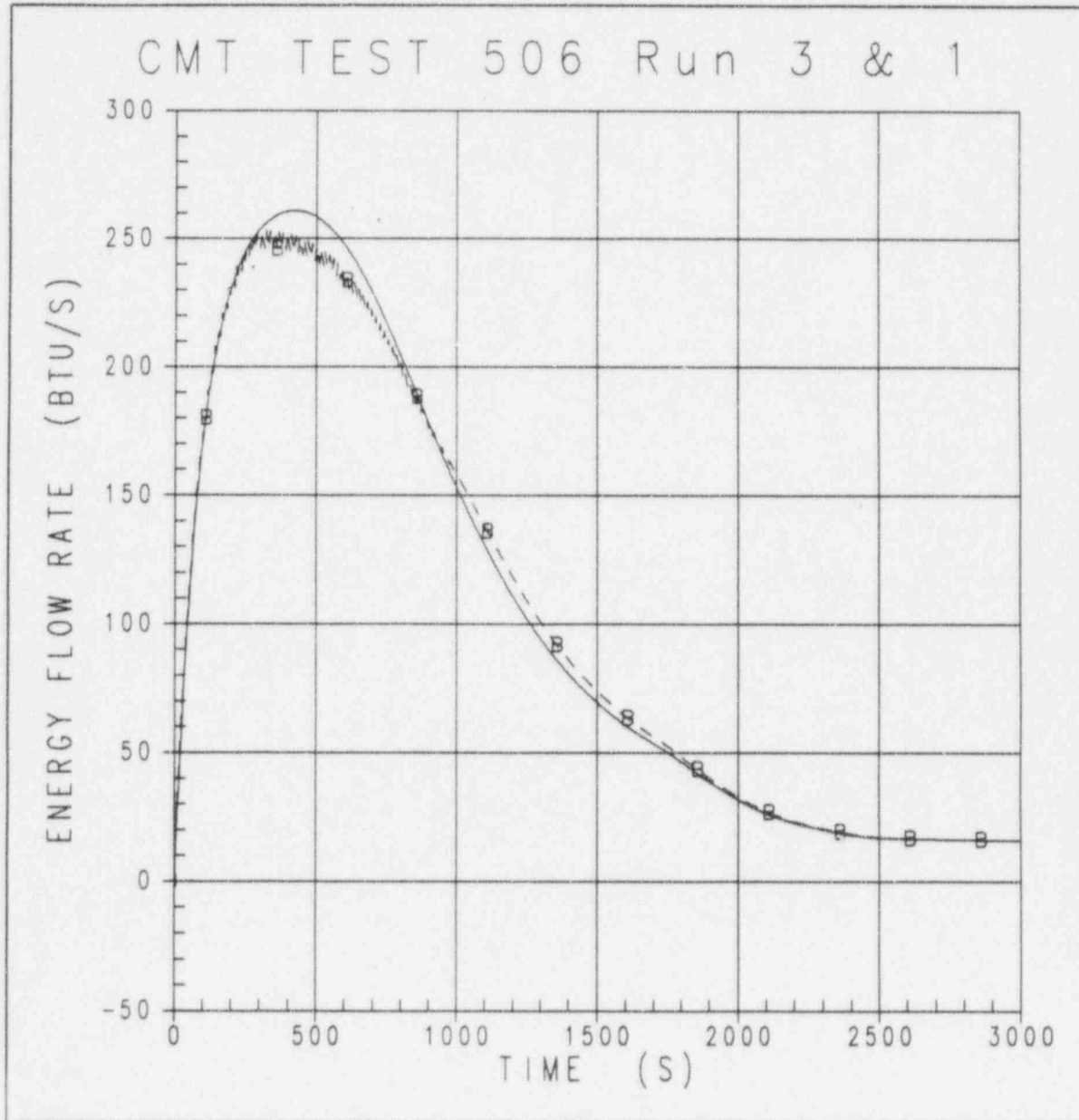B ------  LOFTRANCMT Calculation - Run 1

Westinghouse

**Figure 440.286-2**      C064506 Test, Water-to-Wall Heat Transfer

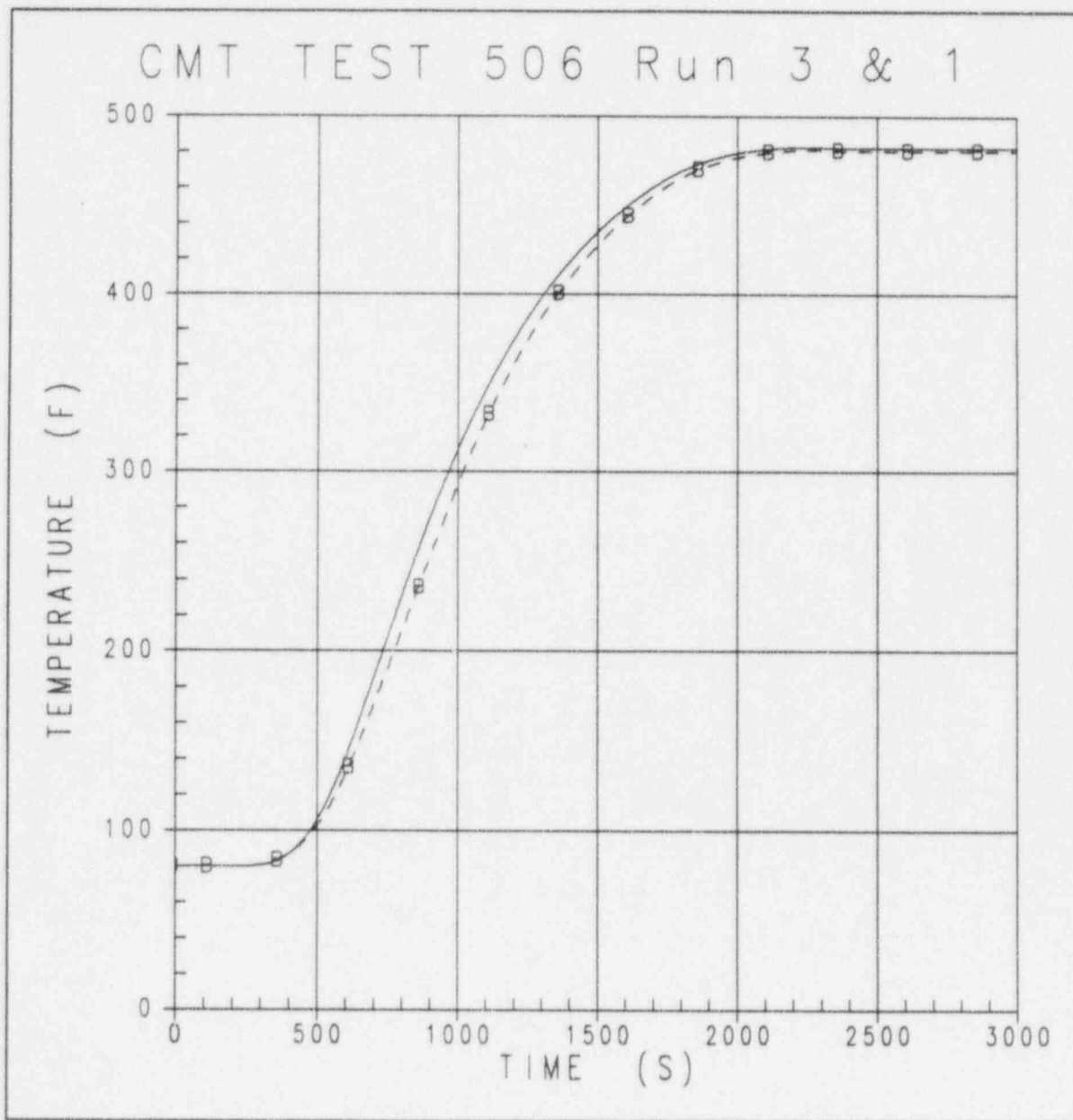_____ LOFTRANCMT Calculation - Run 3
B ----- LOFTRANCMT Calculation - Run 1

AP600



Figure 440.286-3    C064506 Test, CMT Outlet Fluid Temperature
——— LOFTRANCMT Calculation - Run 3
B ----- LOFTRANCMT Calculation - Run 1

Westinghouse
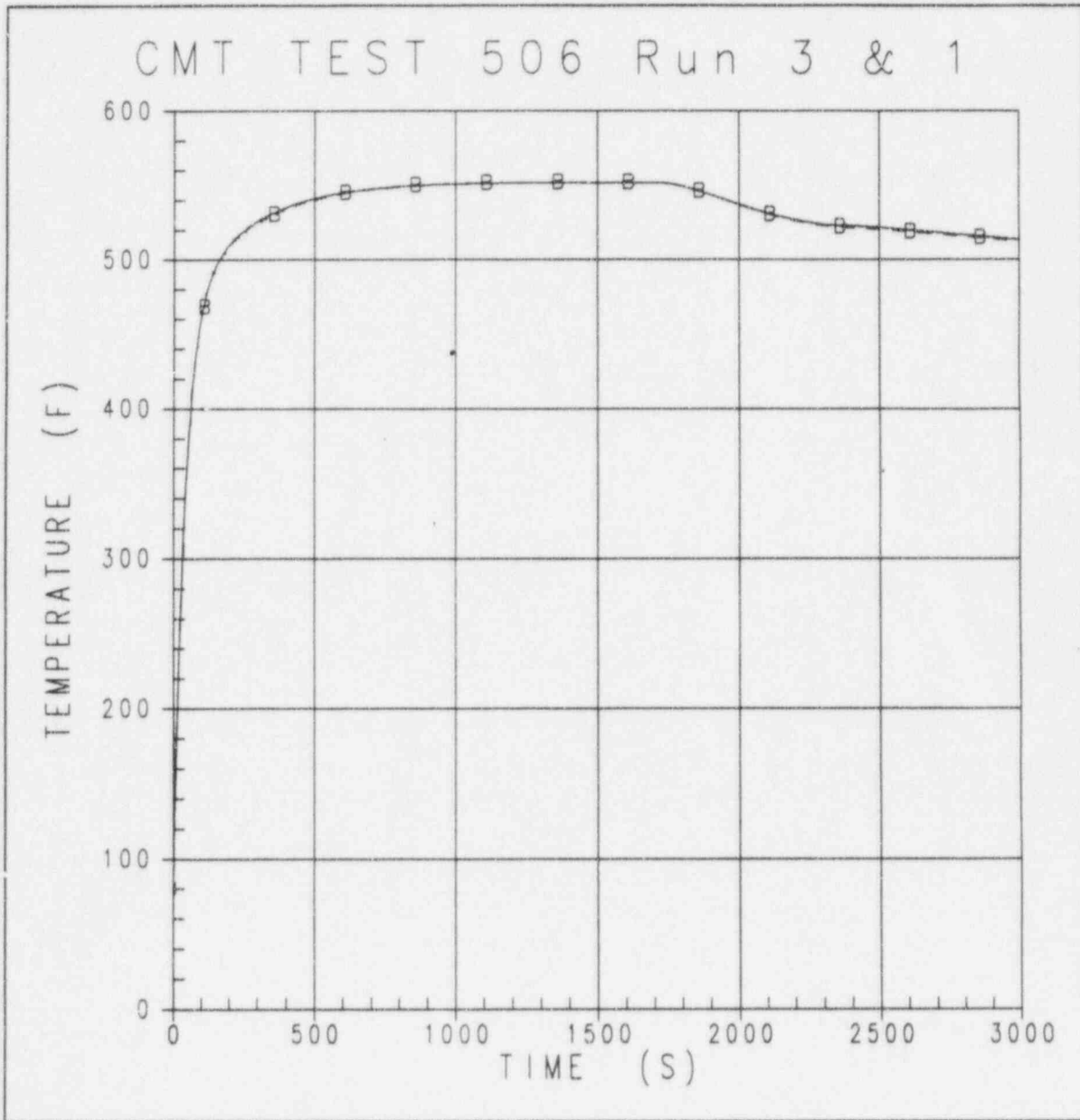
AP600

## CMT TEST 506 Run 3 & 1

Figure 440.286-4    C064506 Test, CMT Fluid Temperature, 4.9 in. From the Top of the CMT

――――  LOFTRANCMT Calculation - Run 3

B ----- LOFTRANCMT Calculation - Run 1

Westinghouse

AP600

CMT TEST 506 Run 3 & 2

Figure 440.286-5    C064506 Test, Injection Line Flow Rate
_____ LOFTRANCMT Calculation - Run 3
B ----- LOFTRANCMT Calculation - Run 2

Westinghouse

Figure 440.286-6    C064506 Test, Water-to-Wall Heat Transfer

_____ LOFTRANCMT Calculation - Run 3

B ----- LOFTRANCMT Calculation - Run 2

Westinghouse

**AP600**



CMT TEST 506 Run 3 & 2

**Figure 440.286-7    C064506 Test, CMT Outlet Fluid Temperature**

_____    LOFTRANCMT Calculation - Run 3

B -----    LOFTRANCMT Calculation - Run 2

Westinghouse
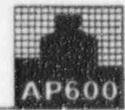
AP600



**CMT TEST 506 Run 3 & 2**

**Figure 440.286-8**     C064506 Test, CMT Fluid Temperature, 4.9 in. From the Top of the CMT

——— LOFTRANCMT Calculation - Run 3

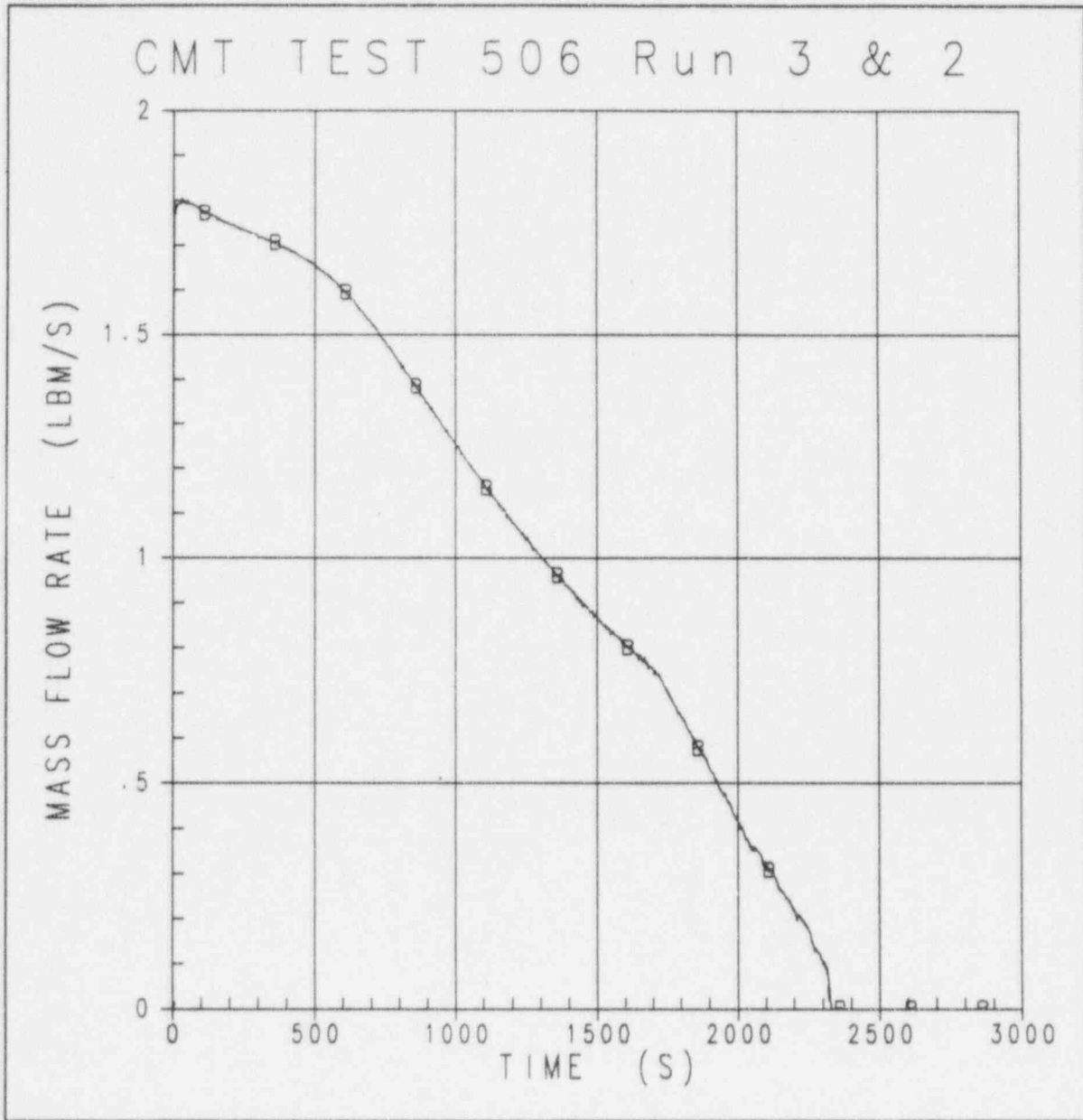B ----- LOFTRANCMT Calculation - Run 2

Westinghouse

440.286-11

NRC REQUEST FOR ADDITIONAL INFORMATION

AP600



**CMT TEST 506 Run 3 & 4**

*(Plot: MASS FLOW RATE (LBM/S) vs TIME (S))*

**Figure 440.286-9**      C064506 Test, Injection Line Flow Rate

    ————     LOFTRANCMT Calculation - Run 3
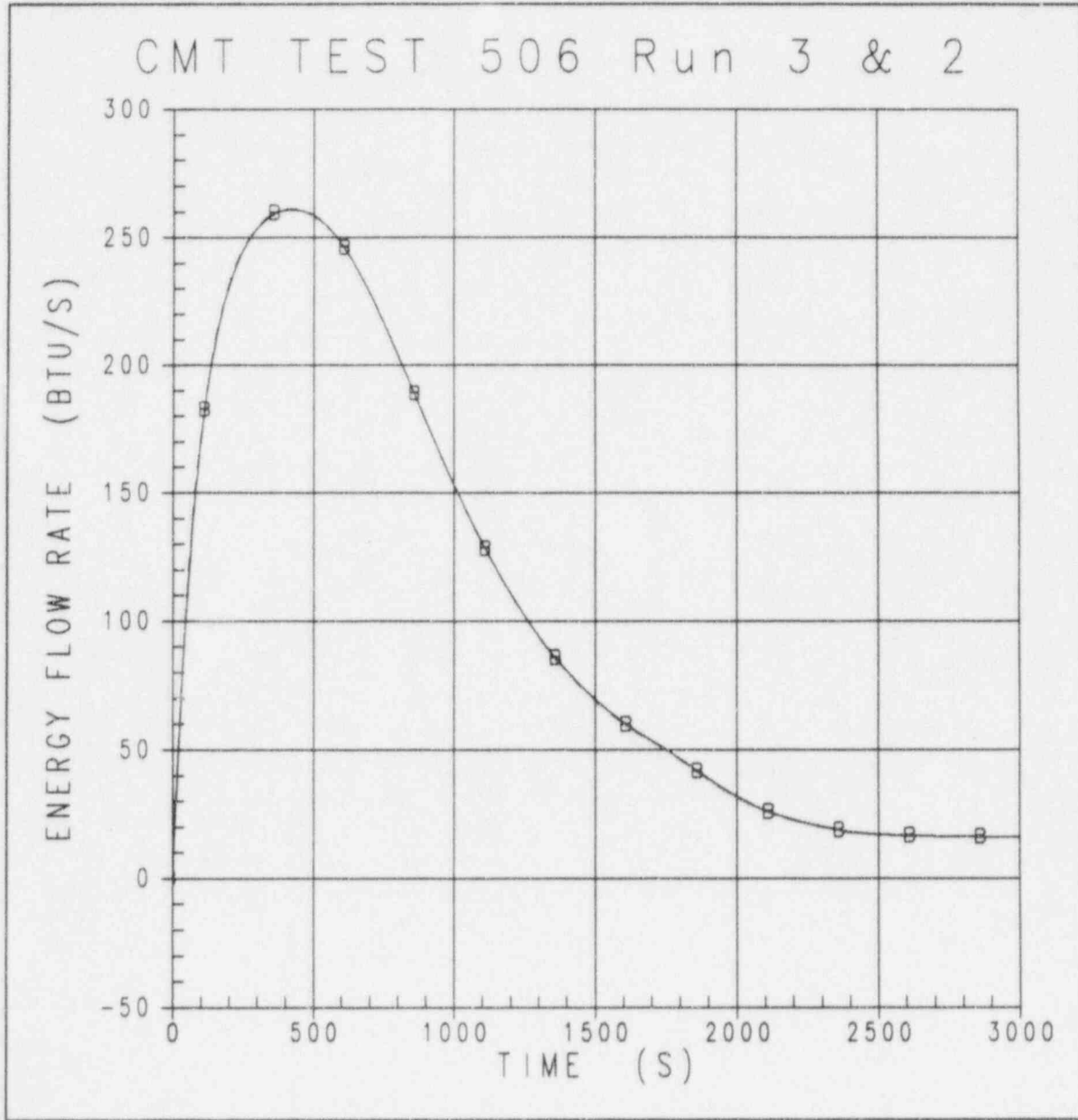B -----     LOFTRANCMT Calculation - Run 4

440.286-12

Westinghouse
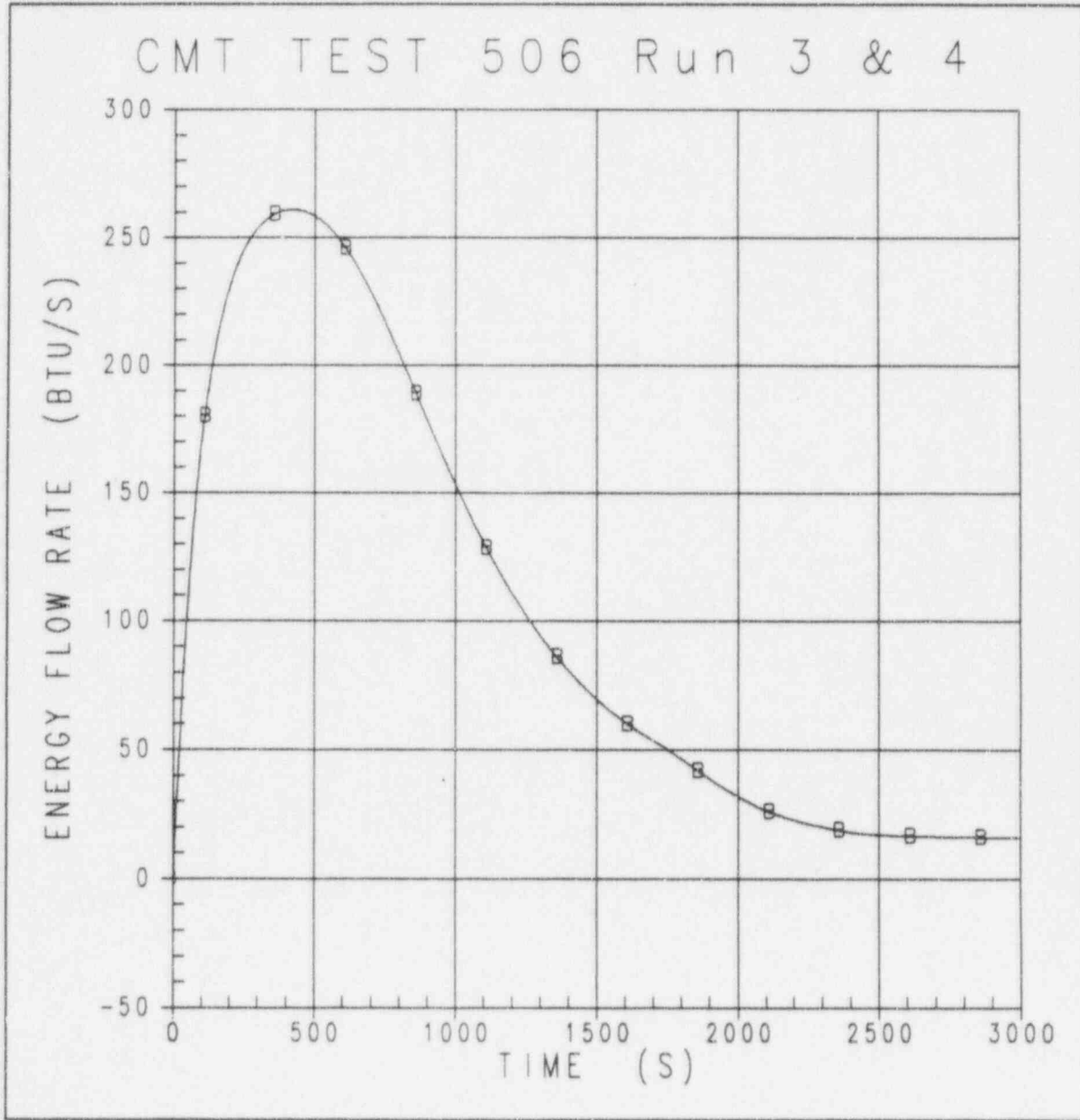
**Figure 440.286-10**      **C064506 Test, Water-to-Wall Heat Transfer**
—— LOFTRANCMT Calculation - Run 3
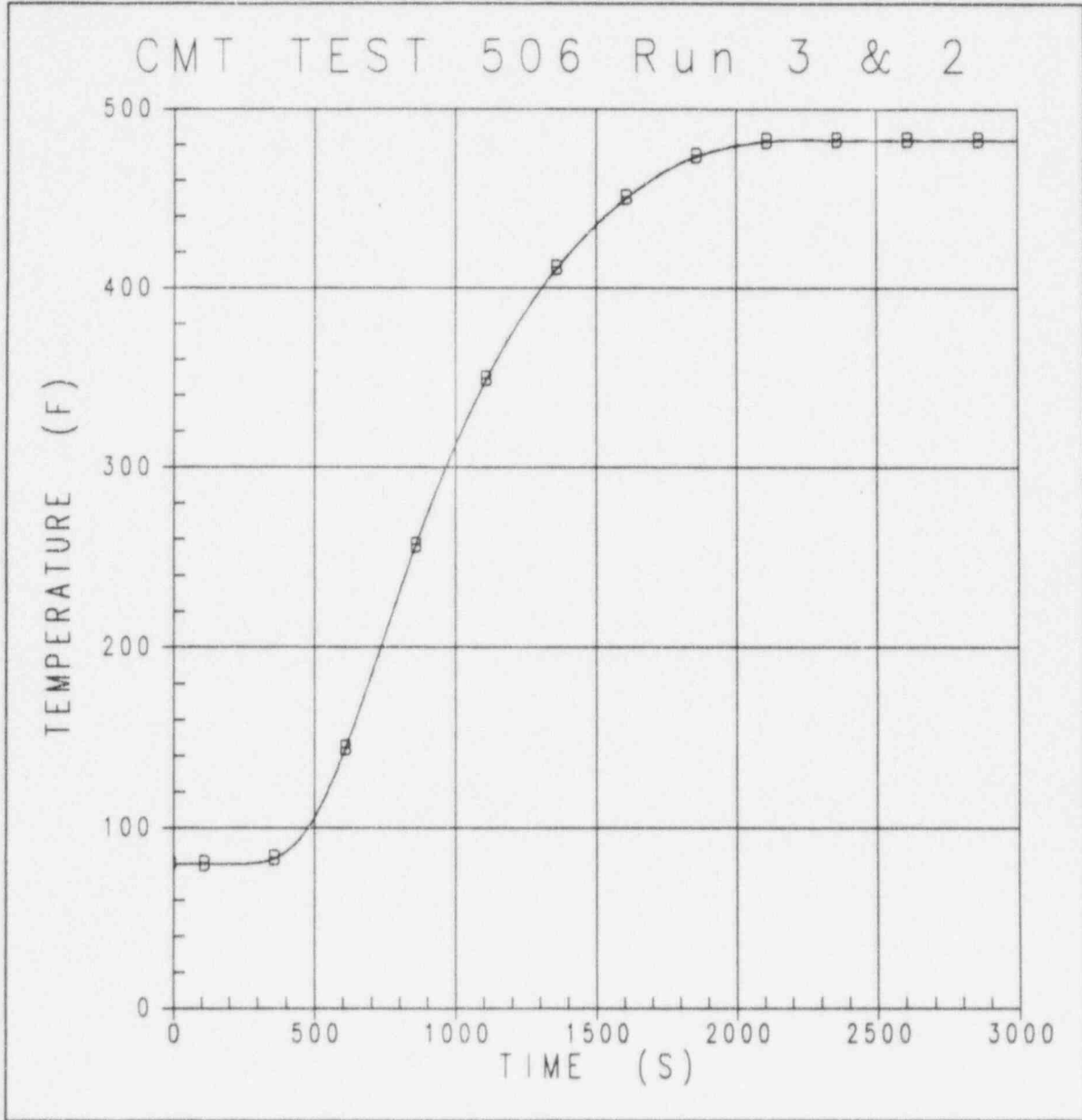B ----- LOFTRANCMT Calculation - Run 4

AP600



**Figure 440.286-11      C064506 Test, CMT Outlet Fluid Temperature**
_____  LOFTRANCMT Calculation - Run 3
B ...... LOFTRANCMT Calculation - Run 4

440.286-14

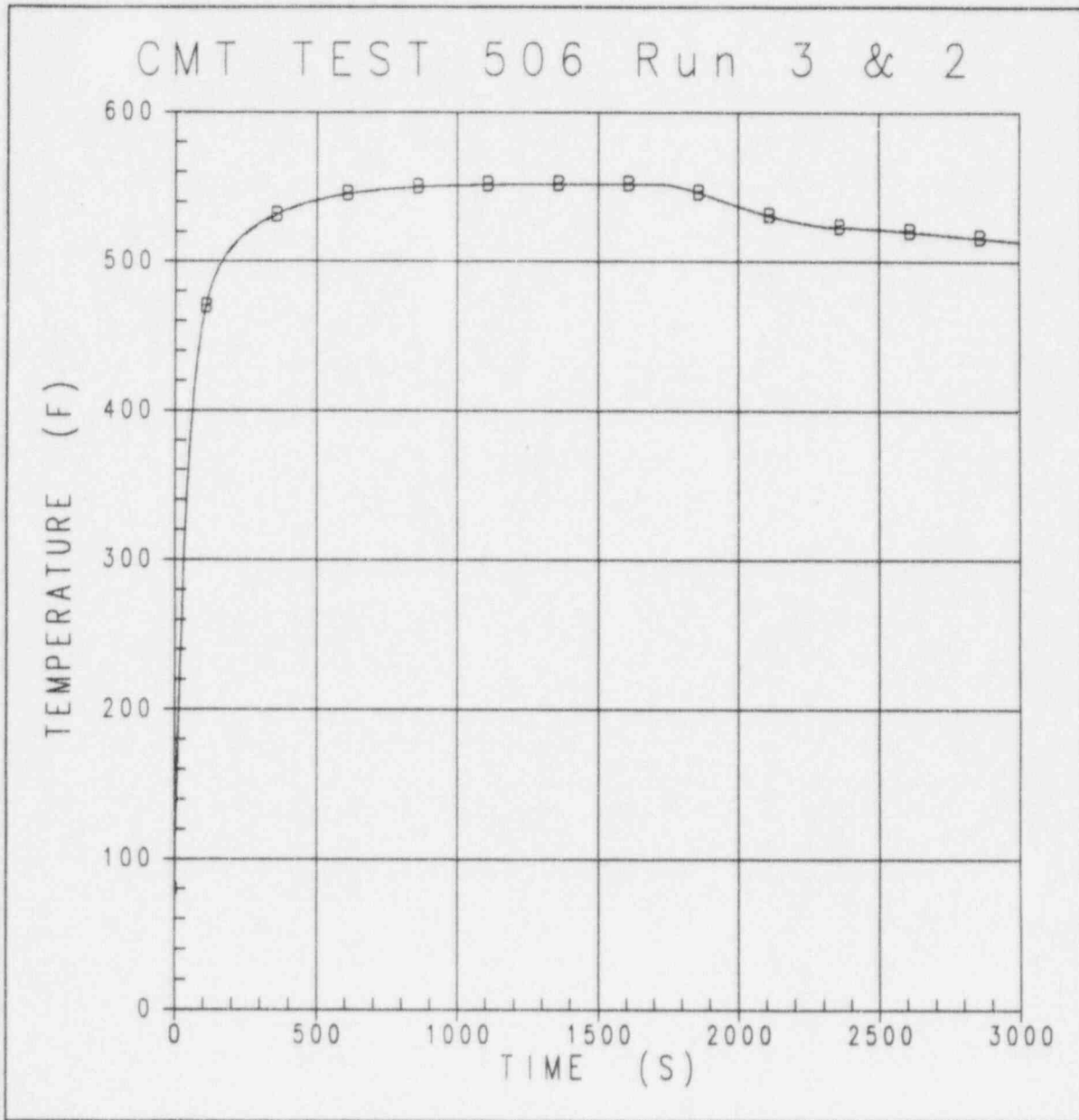Westinghouse

## CMT TEST 506 Run 3 & 4

Figure 440.286-12     C064506 Test, CMT Fluid Temperature, 4.9 in. From the Top of the CMT

_____ LOFTRANCMT Calculation - Run 3
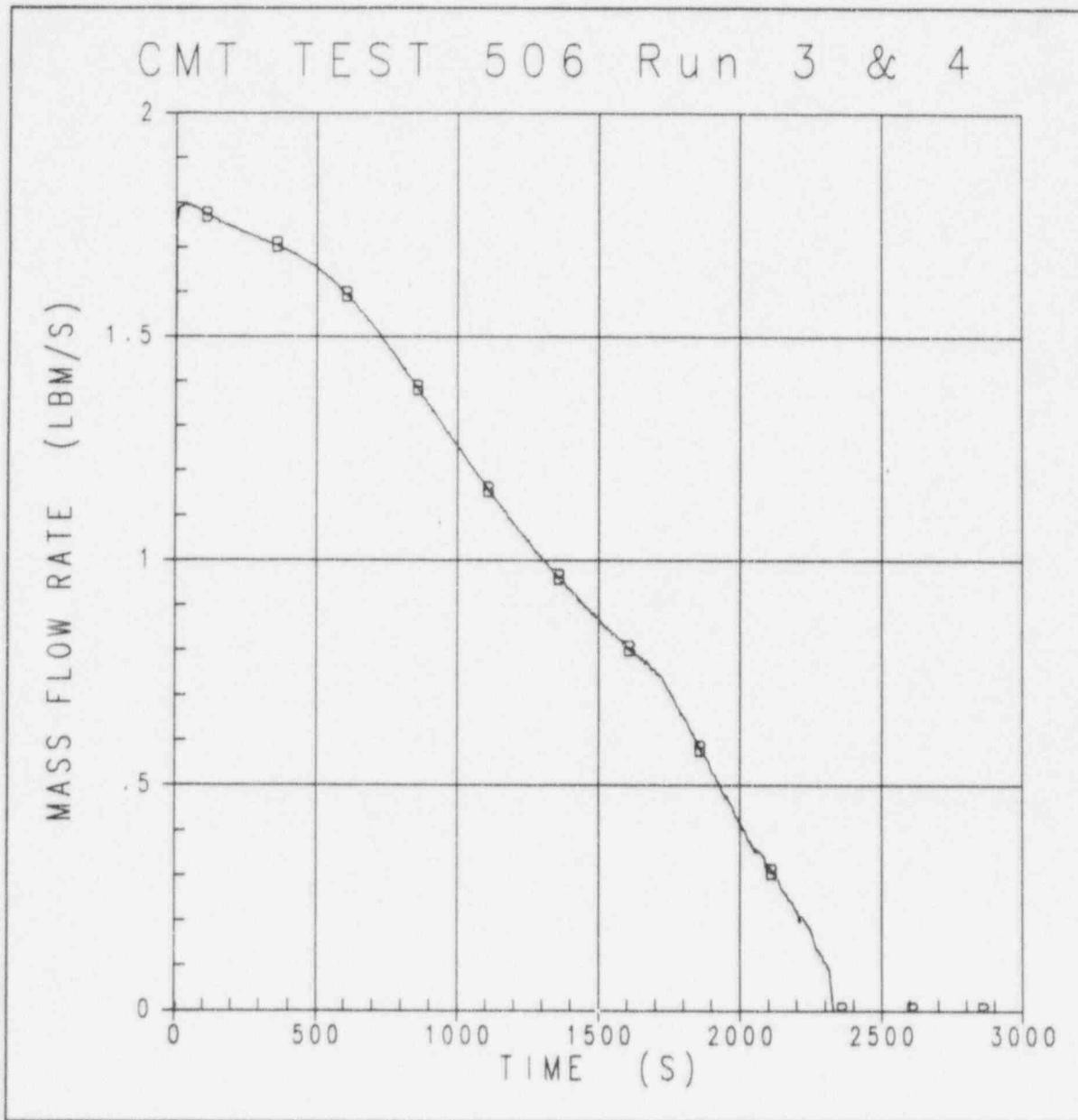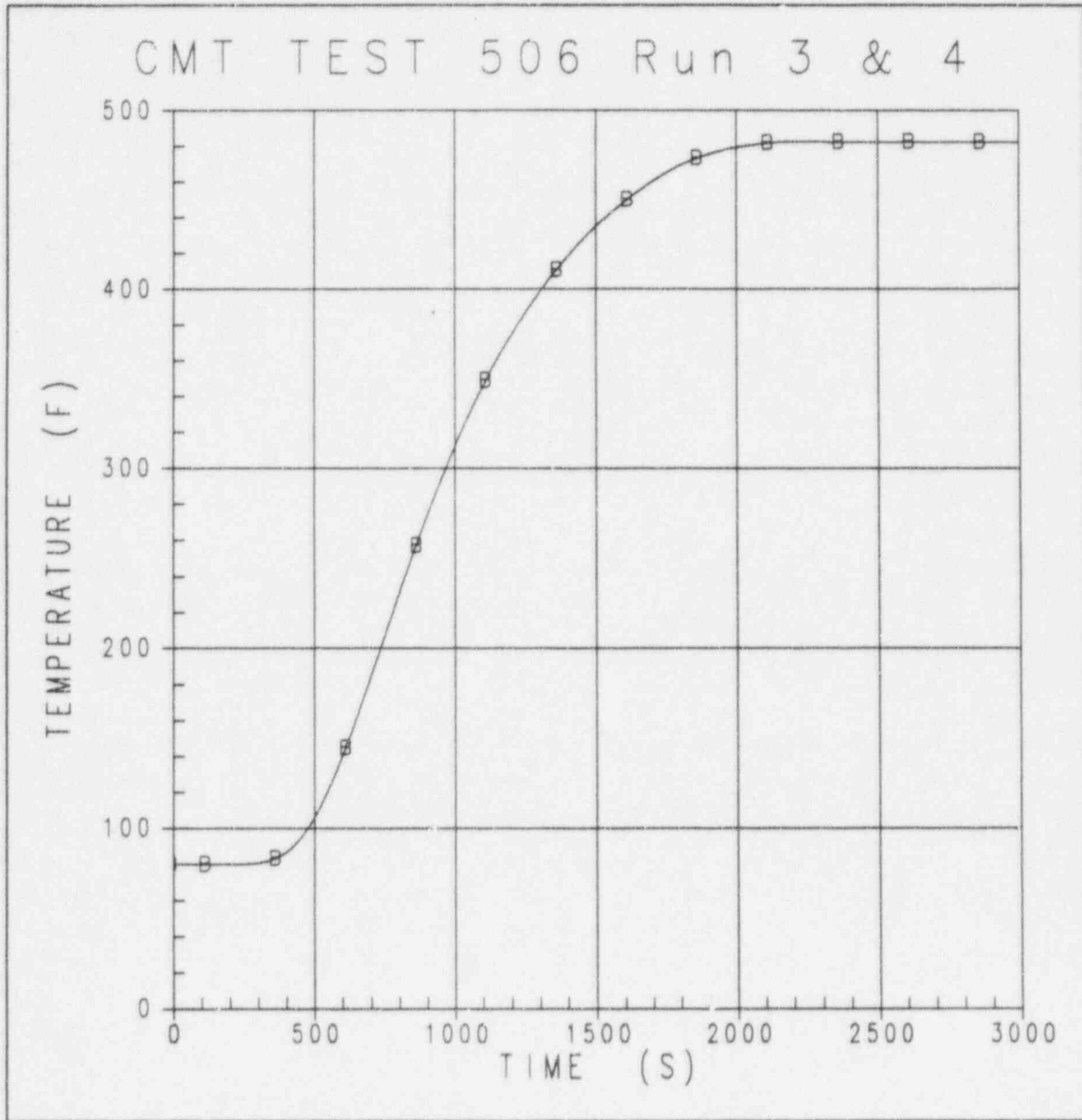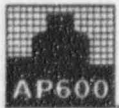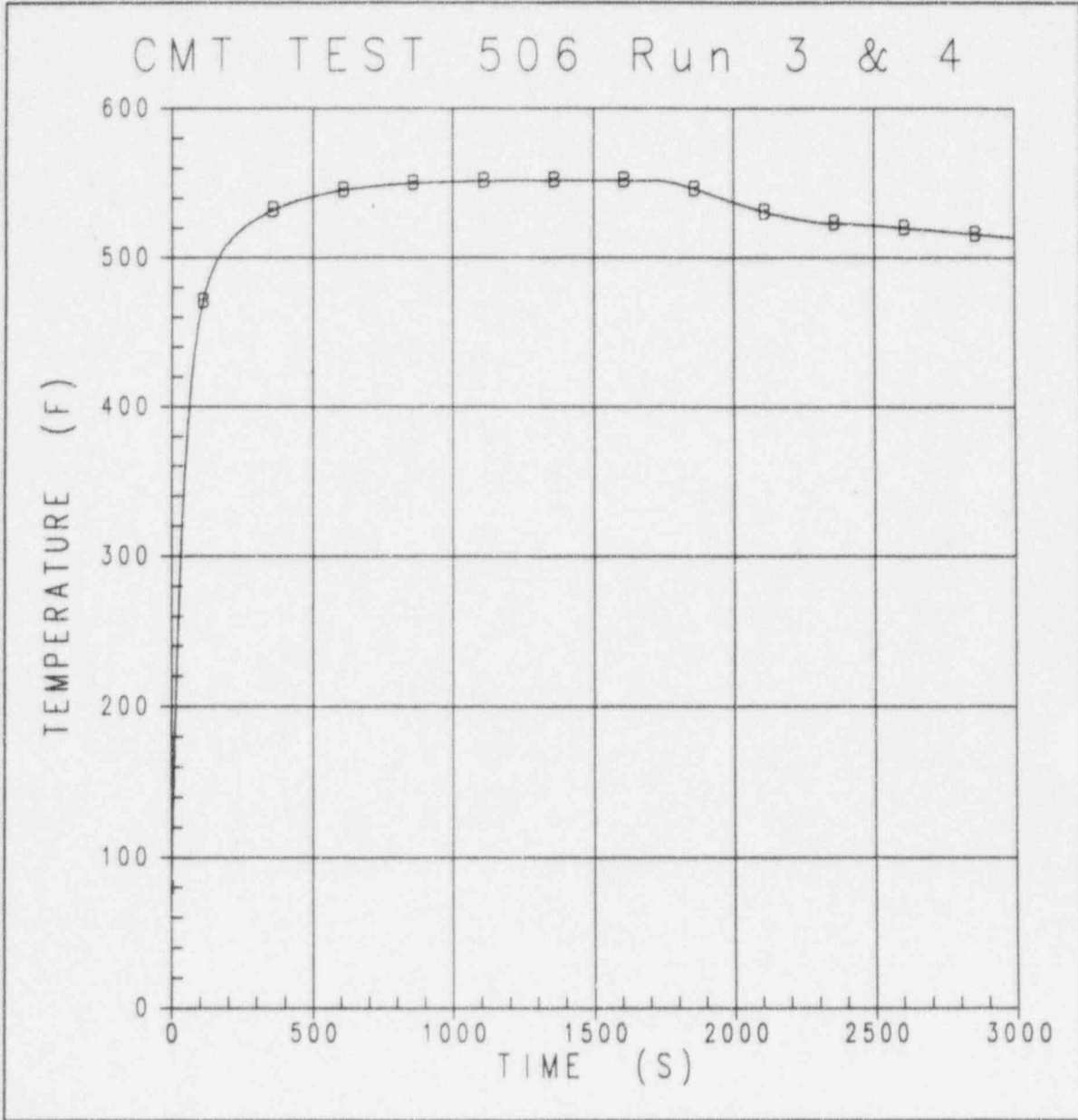B ----- LOFTRANCMT Calculation - Run 4

Westinghouse

440.286-15

Question 440.291

Please provide any details on whether the CMT and the RCS execute at different time steps. If this is the case, please provide the logic that insures both modules reach the same point in time.

Response:

The CMT and the RCS are connected explicitly using the following logic :

1. RCS Flow Calculation

The RCS flow calculations performed by LOFTRAN are used to define the flow in each RCS cell for the new time $(T + DT)$, where DT is the main hydraulic time step size (sec).

2. Boundary Conditions of the CMT for time $T + DT$

The CMT boundary conditions are computed one time per main LOFTRAN time step (DT). The LOFTRAN AP600 CMT model uses three boundary conditions :

$P_{CL}$ = Pressure in cold leg where balance line connects (psi)

$P_{VESSEL}$ = Pressure at CMT injection point in reactor vessel downcomer (psi)

$H_{CL}$ = Enthalpy of water in cold leg where balance line connects (Btu/lbm)

A key point of the connection is that the pressure at the CMT injection point is computed using a single absolute pressure $(P_{CL})$, and the CMT injection point pressure is calculated using:

$$P_{VESSEL} = P_{CL} + (HEIT * \rho_{WC})/144 - \Delta P_{dyn}$$

Where :

HEIT = Altitude from balance line inlet to the CMT injection point in reactor vessel (ft)

$\rho_{WC}$ = Water density in the RCS downcomer (lbm/ft$^3$)

$\Delta P_{dyn}$ = Friction and dynamic pressure loss/recovery through the main RCS piping from balance line connection to injection nozzle (psi). Since the CMT operates after the reactor coolant pumps trip, the RCS flow is small (a few percent of nominal flow), which results in a very small value for $\Delta P_{dyn}$.

3.  CMT Parameter Update

The LOFTRAN CMT module has is own internal time step ($DT_{CMT}$) :

$$DT_{CMT} = DT / N$$

where N is an integer introduced as input data. A typical value for N is five.

For each CMT time step, (i=1 , N), the following sequence is repeated :

3.1 Compute the boundary conditions for the internal time step i of the CMT

The boundary condition pressures are computed assuming a linear evolution during the LOFTRAN Time step DT.

$$P^i = P^t + (i / N) ( P^{t+\Delta t} - P^t )$$

where $\Delta t = DT_{CMT}$

3.2 Perform the CMT Calculations For the Internal Time Step $DT_{CMTi}$

The LOFTRAN CMT module computes the fluid parameters for each node, using the boundary conditions defined above. The CMT wall temperatures are also updated. The inlet balance line flow rate ($W_{CLi}$), the outlet injection line mass flow rate ($W_{INJi}$) and enthalpy ($H_{INJi}$) are stored in memory.

3.3 Compute average mass flow rates and enthalpies

The mass and energy flux for each time step are cumulated during the N CMT time steps, then the following average values are calculated.

$$W_{INJ} = 1/N \; \Sigma \; W_{INJi}$$

$$W_{CL} = 1/N \; \Sigma \; W_{CLi}$$

$$H_{INJ} = [\Sigma \; (W_{INJi} * H_{INJi})] / [\Sigma \; (W_{INJi})]$$

Where:  $W_{INJ}$  =  Average outlet injection line mass flow rate (lbm/sec)

$W_{CL}$  =  Average inlet balance line mass flow rate (lbm/sec)

$H_{INJ}$  =  Average injection line enthalpy (BTU/lbm)

Westinghouse

4.  Update the RCS Fluid at the CMT Connection Points

The RCS to CMT connections are achieved using mass and energy sink and sources :

- Cold leg to CMT connection

    Mass sink :              $-W_{CL} * DT$
    Energy sink :            $- W_{CL} * H_{CL} * DT$

- Downcomer to CMT Connection

    Mass source :            $W_{INJ} * DT$
    Energy source:           $W_{INJ} * H_{INJ} * DT$

The same logic is repeated for each LOFTRAN time step (DT). This logic ensures that the RCS and CMT calculations reach the same point in time.

SSAR Revision: NONE

Question 440.305

Re: LOFTRAN Code Applicability Document (CAD)
Please provide more details in the numerical solution of the heat transfer in the PRHR.

Response:

Pages 3-8 and 3-9 of the CAD (Reference 440.305-1) outline twelve steps followed by the code in evaluating the heat transfer for each PRHR heat exchanger node and for each time step. These steps are elaborated on below, to provide more details on the solution technique. Nomenclature used in this response are collected and defined at the end. All equations have been provided in Appendix A of the CAD.

[1] Calculate primary-fluid temperature in the tube node and the local outside pressure and temperature (pool temperature).

The primary fluid temperature in the node at the start of the timestep is set to the fluid temperature and the end of the previous timestep. The initial IRWST temperature is input by the user and is updated by the code at the end of every timestep to reflect the heat added. The local outside (secondary) pressure for each primary side tube node is calculated at the start of the timestep using the pressure at the top of the tank (containment pressure), with a pressure increase to account for the depth of the node in the tank. The containment pressure can be input by the user as a function of time, although a constant value is typically used. The density of water at the containment pressure and IRWST temperature is used together with the depth of the individual heat exchanger node and the containment pressure to compute the local outside pressure.

[2] Calculate primary-side heat transfer coefficient

The correlation used for the primary side heat transfer coefficient is controlled by user input. The options are Dittus-Boelter and Petkov-Popov. The SSAR analyses use Petkov-Popov. For Dittus-Boelter: The user provides the heat transfer coefficient versus temperature at a references flow rate. The code then adjusts the coefficient for the current flow. For Petkov-Popov: Using the primary side temperature, pressure and mass flux, the code calculates the heat transfer coefficient using the equation presented in the CAD:

$$\overline{h}_c = \frac{K}{D}\overline{Nu_D} = \frac{K\left(\frac{f}{8}Re\,Pr\right)}{D\left[K_1 + K_2\left(\frac{f}{8}\right)^{1/2}(Pr^{2/3} - 1)\right]}$$

440.305-1

Where:

$f$ = friction factor = $(1.82\,Log_{10}Re - 1.64)^{0.2}$
$K_1$ = $1.0 + 3.4f$
$K_1$ = $1.17 + 1.8/Pr^{1/3}$

AP600

The equation for the overall heat transfer coefficient is provided in the CAD:

$$h_t = \cfrac{1}{\cfrac{1}{h_p r_i/r_o} + \cfrac{r_o \log(r_o/r_i)}{K} + \cfrac{1}{h_s} + FF_p + FF_s}$$

440.305-2

Where: $h_t$ = overall heat transfer coefficient, Btu/hr-ft$^2$-°F
$h_p$ = primary-side heat transfer coefficient, Btu/hr-ft$^2$-°F
$h_s$ = secondary-side heat transfer coefficient, Btu/hr-ft$^2$-°F
$K$ = PRHR tube metal conductivity, Btu/hr-ft-°F
$r_i$ = inner radius of the PRHR tube, ft
$r_o$ = outer radius of the PRHR tube, ft
$FF_p$ & $FF_s$ = primary-side and secondary-side tube fouling factors, hr-ft$^2$-°F/Btu

The inner and outer radii are user input, as are the primary and secondary fouling factors. The tube metal conductivity is input by the user as a function of tube wall temperature. The average of the primary fluid temperature (inside surface) and the IRWST temperature (outside surface) is used to determine this conductivity. This is an acceptable approximation since the tube walls are thin and the actual variation of the conductivity with temperature is small (on the order of $5 \times 10^{-3}$ Btu/hr-ft$^2$-°F per °F).

Once the primary side heat transfer coefficient, the tube metal conductivity and fouling factors are determined, the only term remaining in the above equation for the overall heat transfer coefficient is the secondary side heat transfer coefficient, calculated in Step 3 below.

[3] Calculate the secondary-side heat transfer coefficient and heat flux using the natural convection heat transfer correlation

The user specifies which heat transfer correlations will be used in evaluating the secondary side heat transfer coefficient. For convection the options are McAdams and Eckert-Jackson. For the SSAR Chapter 15 analyses, Eckert-Jackson was used. The user has the option to bypass the natural convection heat transfer calculations thereby forcing the code to evaluate the heat transfer using pool boiling heat transfer.

For McAdams:

For vertical tubes the equation is presented in the CAD:

$$\overline{h}_c = 0.13K \left( \frac{g \beta Pr}{v^2} \right)^{1/3} \Delta T^{1/3}$$

440.305-3

Westinghouse
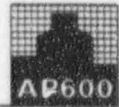
For horizontal tubes the equation presented in the CAD is:

$$\overline{Nu_D} = \frac{\overline{h_c}D}{K} = 0.53(Gr_D PR)^{1/4}$$

440.305-4

By solving for the heat transfer coefficient and substituting for $GR_D$ the equation becomes:

$$\overline{h_c} = 0.53\left(\frac{g\beta PR}{v^2}\right)^{1/4} \Delta T^{1/4}$$

440.305-5

Where:
$\Delta T$ = outer tube wall temperature ($T_{wall}$) minus the pool water temperature ($T_{pool}$), °F. The wall properties are calculated at an average film temperature defined as: $T_{avg} = (T_{wall} + T_{pool})/2$.

For Eckert-Jackson the equation from the CAD is:

$$h_c(x) = \frac{6}{5}0.021\frac{K}{x}(Gr_x Pr)^{2/5}$$

440.305-6

Substituting for $Gr_x$ the equation becomes:

$$h_c(x) = \frac{6}{5}0.021K\left(\frac{g\beta Pr}{v^2}\right)^{2/5} x^{1/5} \Delta T^{2/5}$$

440.305-7

The above equations for the secondary side heat transfer coefficient provide the missing secondary side heat transfer coefficient from the equation 440.305-2. The equation can be simplified by grouping the components of the total heat transfer coefficient into two groups. The first group accounts for the heat transfer coefficient up to the outer tube wall and the other is the heat transfer coefficient at the outer tube wall:

$$h_t = \cfrac{1}{\cfrac{1}{h_p r_i/r_o} + \cfrac{r_o \log(r_o/r_i)}{K} + \cfrac{1}{h_s} + FF_p + FF_s}$$

$$h_t = \cfrac{1}{F + \cfrac{1}{h_s}}$$

$$h_t = \cfrac{h_s \frac{1}{F}}{h_s + \frac{1}{F}}$$  440.305-8

Where F represents all the contributors to the total heat transfer coefficient except for the secondary side film heat transfer coefficient. With this expression it is a simple matter to determine the total heat transfer coefficient with the selected secondary side convective heat transfer correlation and from there evaluate the heat flux.

In the above secondary side heat transfer coefficient calculations (McAdams & Eckert-Jackson) outside tube wall and secondary side film temperatures are required. An initial estimate at the temperature of the tube wall and the film outside the tubes is obtained using an estimate at the heat flux and applying an initial estimate of the secondary side heat transfer coefficient, $h_s$. The initial estimate of $h_s$ is F, the total heat transfer coefficient in equation 440.305-2, neglecting the contribution of the secondary side coefficient.

$$\Delta T_{estimate} = \frac{q_{estimate}}{F}$$  440.305-9

where $\Delta T_{estimate}$ represents the difference between the outside wall temperature and the pool fluid temperature on which the heat flux is based. From this heat flux and $h_s$ estimate, the wall and film temperatures are obtained. $[T_{pool} = T_{wall} - \Delta T_{estimate}$ and $T_{film} = (T_{wall} + T_{pool})/2]$.

The McAdams or Eckert-Jackson equations are then used to compute the first approximate value of the secondary side heat transfer coefficient assuming these first guess values for wall and film temperatures (based on the first estimate of the heat flux and $h_s$).

Westinghouse

The approximate secondary side heat transfer coefficient is tested by applying the $\Delta T = q/h$ equation but this time using the calculated secondary heat transfer coefficient. The resulting heat flux is compared to the heat flux estimate. If the calculated heat flux and the estimated heat flux are within 1%, then the secondary side heat transfer coefficient is accepted (together with the heat flux and wall and film temperatures). If not, the computed heat flux is used together with the initial estimate to get a new estimate at the heat flux and the process is repeated, with the calculated approximate $h_s$ replacing F in equation 440.305-9, until the calculated heat flux matches the estimated heat flux (within 1%).

[4] Calculate the secondary-side heat transfer coefficient using the pool boiling heat transfer correlation

The user specifies which heat transfer correlations will be used in evaluating the secondary side pool boiling heat transfer coefficient. [Both heat transfer equations are in the form $q = a\Delta T^b$.]

For Rohsenow: The user provides the multiplier "a" (in the heat flux equation) as a function of the local secondary pressure. The exponent $b = 3$.

For PRHR Experimental: The user inputs constant "a" multipliers and "b" exponents for vertical and horizontal nodes. This option is used in the SSAR Chapter 15 analyses.

An initial estimate at the temperature of the tube wall and the temperature of the film outside the tubes is obtained using an estimated heat flux and manipulating the boiling heat transfer equation.

$$q_{estimate} = a\left(\Delta T_{estimate}\right)^b$$

$$\left(\Delta T_{estimate}\right)^b = \frac{1}{a}q_{estimate}$$

$$\Delta T_{estimate} = \frac{1}{a}^{\frac{1}{b}}\left(q_{estimate}\right)^{\frac{1}{b}} \qquad\qquad 440.305\text{-}10$$

where $\Delta T_{estimate}$ represents the difference between the outside wall temperature and the saturation temperature of the pool fluid ($T_{sat}$) on which the heat flux is based. From this heat flux estimate, the wall and film temperatures are obtained. [$T_{pool} = T_{wall} - \Delta T_{estimate}$ and $T_{film} = (T_{wall} + T_{pool})/2$].

The updated wall and film temperatures are used to compute a new heat flux. The resulting heat flux is compared to the estimated heat flux. If the calculated heat flux and the estimated heat flux are within 1% then the pool boiling heat flux is accepted (together with the wall and film temperatures). If not the computed heat flux is used together with the initial estimate to get a new estimate of the heat flux and the process is repeated until the calculated heat flux matches the estimated heat flux (within 1%).

AP600

[5] Assume the heat transfer mode related to the higher heat flux of Steps 3 and 4.

All of the components of the total heat transfer coefficient equation (440.305-2) above,

$$h_t = \cfrac{1}{\cfrac{1}{h_p r_i/r_o} + \cfrac{r_o \log(r_o/r_i)}{K} + \cfrac{1}{h_s} + FF_p + FF_s}$$

are now available. $h_s$ takes on the value associated with the secondary heat transfer mode that produces the higher heat flux.

[6] Calculate the total heat transfer coefficient and evaluate the heat flux by applying the related $\Delta T$.

The total primary to secondary heat transfer for the node is calculated depending on which secondary side heat transfer mode results in higher heat flux.

For convective heat transfer: $Q = A/h_t(T_{primary} - T_{secondary})$

For boiling heat transfer: $Q = A/h_t(T_{primary} - T_{sat-secondary})$

[7] Calculate critical heat flux

The critical heat flux is calculated using either the Griffith or Berensen CHF formulas as specified by the user. The SSAR Chapter 15 analyses used Griffith.

$$CHF_G = 0.9(1 - \alpha)\frac{\pi}{23}h_{fg}\,\rho_g^{0.5}\left[g\,g_c\,\sigma(\rho_f - \rho_g)\right]^{0.25} \qquad 440.305\text{-}11$$

or

$$CHF_B = \frac{CHF_G}{0.9}\left(\frac{\rho_f}{\rho_f - \rho_g}\right)^{0.25} \qquad 440.305\text{-}12$$

Where:  $CHF_G$ = Griffith critical heat flux, Btu/hr-ft$^2$
   $CHF_B$ = Berensen critical heat flux, Btu/hr-ft$^2$
   $\alpha$ = IRWST void fraction

As described in the CAD an option is included in the code to add Zuber's correction to the Griffith or Berensen critical heat flux calculations. The correction is implemented in LOFTRAN and LOFTTR2 (assuming atmospheric pressure and 100°F) as:

Westinghouse
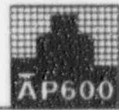
$$\frac{q_{crit-subcooled}}{q_{crit-saturated}} = 1.0 + (QSUBCR)\,(0.0263)\,(T_{sat} - T_{pool}) \qquad 440.305\text{-}13$$

Where: QSUBCR is a user input adjustment factor. For the SSAR Chapter 15 analyses, the Zuber correction was not used. It is intended that a QSUBCR value of 1.0 will be used if conditions warrant application of the Zuber correction.

Once the critical heat flux is calculated the outer wall temperature assuming critical heat flux is obtained for future use. Both the Rohsenow and PRHR Experimental correlations have the same form which is used to obtain the wall temperature as a function of the critical heat flux (and input coefficients) as:

$$\Delta T = \frac{1}{a}^{\frac{1}{b}}(q)^{\frac{1}{b}}$$

$$T_{wall} - T_{sat} = \frac{1}{a}^{\frac{1}{b}}(q)^{\frac{1}{b}}$$

$$T_{wall} = T_{sat} + \frac{1}{a}^{\frac{1}{b}}(q)^{\frac{1}{b}} \qquad 440.305\text{-}14$$

[8] If the calculated heat flux (from Step 6) is less than the critical heat flux (from Step 7), then the calculated heat flux is accepted and the calculation is finished; otherwise, the following steps (9 through 12) are performed.

[9] Evaluate the minimum temperature for stable film boiling ($T_{MSFB}$).

The minimum stable film boiling point ($T_{MSFB}$) is calculated as the minimum of $T_{min}(1)$ and $T_{min}(2)$ where:

$$T_{min}(1) = T_{HN} + (T_{HN} - T_{l})\sqrt{\frac{(K\,\rho\,C_{p})_{l}}{(K\,\rho\,C_{p})_{wall}}} \qquad 440.305\text{-}15$$

and

$$T_{min}(2) = T_{B} + 0.42\,(T_{B} - T_{l})\left[\sqrt{\frac{(K\,\rho\,C_{p})_{l}}{(K\,\rho\,C_{p})_{wall}}}\left(\frac{h_{fg}}{C_{p\,wall}\,(T_{B} - T_{l})}\right)\right]^{0.6} \qquad 440.305\text{-}16$$

Where:

AP600

$$T_B = T_1 + 0.127 \frac{\rho_g h_{fg}}{K_g} \left[ \frac{g(\rho_f - \rho_g)}{(\rho_f + \rho_g)} \right]^{2/3} \left[ \frac{g_c \sigma}{g(\rho_f - \rho_g)} \right]^{1/2} \left[ \frac{\mu_g}{g(\rho_f - \rho_g)} \right]^{1/3}$$

440.305-17

Where: P $=$ IRWST local pressure, psia

DP $=$ 3203.6 - P

$T_{HN}$ $=$ Homogeneous nucleation temperature

$=$ 705.44 - 4.772x10$^{-2}$DP + 2.3907x10$^{-5}$DP$^2$ - 5.8193x10$^{-9}$DP$^3$

$T_1$ $=$ saturation temperature at local IRWST pressure, °F

$(K\rho C_p)_{wall}$ $=$ product of thermal conductivity (Btu/hr-ft-°F), density (lbm/ft$^3$) and specific heat of PRHR tube wall (Btu/lbm-°F)

$(K\rho C_p)_1$ $=$ product of thermal conductivity (Btu/hr-ft-°F), density (lbm/ft$^3$) and specific heat of saturated liquid (Btu/lbm-°F) at the local IRWST pressure

$C_{p\,wall}$ $=$ specific heat of PRHR tube wall (Btu/lbm-°F)

and $h_{fg}$, $\rho_f$, $\rho_g$ $K_g$ and $\mu_g$ are evaluated at the local IRWST pressure.

[10] Evaluate the outer tube wall temperature ($T_{OUT}$).

This step determines the outer wall temperature assuming stable film boiling. The film boiling heat flux at the outer wall surface is calculated with the Bromley-Pomeranz correlation equation assuming that the wall temperature $T_w$ is at $T_{MSFB}$.

$$q = 0.62 + \left[ \frac{D}{\lambda_c} \right]^{0.172} \left[ \frac{K_g^3 \rho_g (\rho_f - \rho_g) h'_{fg} g}{D \mu_g (T_w + T_{sat})} \right]^{1/4} (T_w - T_{sat})$$

440.305-18

where:

$$\lambda_c \equiv 2\pi \left[ \frac{g_c \sigma}{g(\rho_f - \rho_g)} \right]^{1/2}$$

440.305-19

and

$$h'_{fg} \equiv h_{fg} \left[ 1.0 + 0.4 C_{pg} \frac{(T_w - T_{sat})}{h_{fg}} \right]$$

440.305-20

The saturation properties $T_{sat}$, $h_{fg}$, $\rho_f$, $\rho_g$, $\mu_g$ and $C_{pg}$ are evaluated at the local IRWST pressure. Surface tension ($\sigma$) is evaluated at $T_{sat}$. [Note that in the CAD the right bracket in the $\lambda_c$ equation is missing and the exponent is misplaced.]

Westinghouse

AP600

This same heat flux exists on the primary side up to the outer wall. Using the film boiling heat flux and the heat transfer coefficient up to the outer wall (including fouling etc.), the wall outer temperature can be obtained:

$$q = \frac{\Delta T}{F}$$

$$\Delta T = qF$$

$$T_{primary} - T_{out} = qF$$

$$T_{out} = T_{primary} - qF \qquad\qquad 440.305\text{-}21$$

[11] If $T_{MSFB} < T_{OUT}$, then the secondary side heat transfer coefficient is assumed to be the Bromley heat transfer coefficient.

The stable film boiling heat flux (Bromley-Pomeranz) was calculated in the previous step. The heat transfer coefficient is backed out manipulating $q = h\Delta T$ into $h = q/\Delta T$, where $\Delta T$ is $T_{MSFB} - T_{sat}$ of the pool.

[12] If $T_{MSFB} \geq T_{OUT}$, then evaluate the secondary side heat transfer coefficient by interpolating between the critical heat flux and the Bromley heat flux.

The equations for this interpolation are provided in the CAD using the wall temperature calculated in Step 7 assuming critical heat flux and the wall temperature calculated in Step 10 assuming stable film boiling.

$$Q_{TB} = \delta\, Q_{CHF} + (1 - \delta)\, Q_{MSFB} \qquad\qquad 440.305\text{-}22$$

where:

$$\delta \equiv \left[ \frac{(T_{wall} - T_{MSFB})}{(T_{CHF} - T_{MSFB})} \right]^2 \qquad\qquad 440.305\text{-}23$$

The calculated secondary side heat transfer coefficient from Step 3 (convection), Step 4 (pool boiling) Step 10 (critical heat flux), Step 11 (stable film boiling) or Step 12 (transition boiling) is then used together with the primary side heat transfer coefficient and fouling factors etc. to obtain the total heat transfer coefficient and calculate the nodes heat transfer and final nodal fluid and wall temperatures.

Westinghouse

440.305-9

AP600

After Step 12

Once the heat transfer from the node has been calculated the new condition in the node is evaluated. If the change in primary fluid temperature is more than 2°F, then the entire calculation for the nodes heat transfer is redone assuming a revised primary temperature for the heat transfer calculations. The primary temperature is estimated at the average of the temperature from the previous timestep and the value calculated using the above steps.

Westinghouse

Nomenclature:

$C_p$ = Fluid heat capacity (Btu/lbm-°F)

$D$ = Equivalent tube diameter (ft)

$\overline{h}_c$ = Average heat transfer coefficient (Btu/hr-ft²-°F)

$h$ = Fluid enthalpy (Btu/lbm)

$g$ = Gravitational acceleration = $4.17 \times 10^8$ (ft/hr²)

$g_c$ = Conversion factor = $4.17 \times 10^8$ (lbm-ft/lbf-hr²)

$Gr$ = Grashof number

$$Gr_L = (g\beta/v^2)L^3 \Delta T$$
$$Gr_D = (g\beta/v^2)D^3 \Delta T$$
$$Gr_x = (g\beta/v^2)x^3 \Delta T$$

$K$ = Fluid thermal conductivity (Btu/hr-ft-°F)

$L$ = Length of heated surface (ft)

$Nu$ = Nusselt number

$$\overline{Nu_D} = \overline{h}_c D/K$$
$$\overline{Nu_L} = \overline{h}_c L/K$$

$Pr$ = Prandlt number = $C_p \mu/K$

$Re$ = Reynolds number = $Dv\rho/\mu$

$v$ = Velocity of water in tubes (ft/hr)

$x$ = Distance from bottom of heat exchanger (ft)

$\beta$ = Thermal expansion factor = $-(1/\rho)(\delta\rho/\delta T)_p$

$\mu$ = Fluid viscosity (lbm/ft-hr)

$\rho$ = Fluid density (lbm/ft³)

$\sigma$ = Surface tension of liquid to vapor interface (lbf/ft)

$v$ = kinematic viscosity = $\mu/\rho$ (ft²/hr)


Subscripts

f = Properties of saturated liquid

g = Properties of saturated vapor

fg = Increment in quantity for evaporation from liquid to vapor

**AP600**

References

440.305-1     WCAP-14234, "LOFTRAN & LOFTTR2 AP600 Code Applicability Document", November 1994.

SSAR Revision: NONE

Question 440.361

Re: CMT Final Data Report and Final Test Analysis Report
The CONTRA model used by Westinghouse is apparently a modified version of the CONTA model developed by Sandia National Laboratory (SNL). If this is correct, provide documentation describing how the SNL model was modified, validation of the modifications, and benchmarking of the modified model to known heat flux data.

Response:

The CONTRA model used in the analysis of the CMT tests is a modified version of the CONTA program which was originally developed by SANDIA. CONTA is written as a one-dimensional rectangular co-ordinate inverse conduction program and a radial inverse conduction program for solid cylinders of infinite length. The changes made were to model an annular geometry in which different time dependent boundary conditions could be imposed on either the inner or the outer surface. The changes to the CONTA program for annular geometries were verified against calculations using the general purpose finite element heat transfer program called ANSYS (Reference 440.361-1 ). A number of test cases were performed using the ANSYS program with step increases in temperature, or in heat transfer coefficient from a given initial condition. The ANSYS program calculated the transient temperature distribution that was used in the CONTRA program as input data. CONTRA then calculated the wall heat transfer coefficient or surface temperature which had been assumed in the ANSYS calculation. A flow chart of the process is given in Figure 440.361-1. The results of the comparisons for a constant heat transfer coefficient of 500 Btu/hr-ft**2 with a surface temperature ramp from 70 °F to 650 °F are shown in Figures 440.361-2 to 440.361-4. The agreement is excellent indicating that the inverse calculation by CONTRA reproduces the imposed heat flux and heat transfer coefficient for the CMT tests.

References:

440.361-1   ANSYS - Engineering Analysis System Manual, Version 5.1 (1995) Swanson Analysis Systems Inc., Houston, Pa.
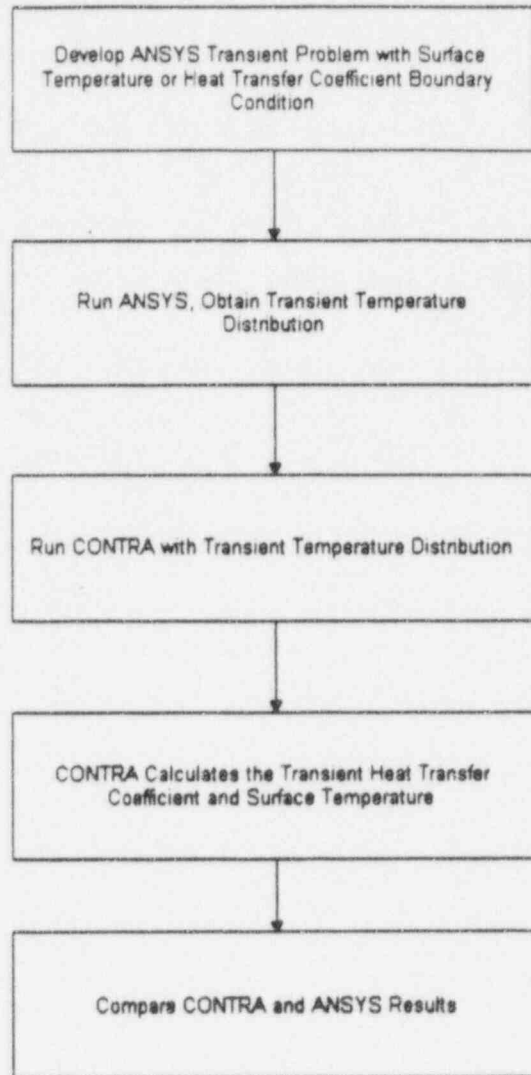
SSAR Revision: NONE

AP600

```
┌─────────────────────────────────────────────┐
│   Develop ANSYS Transient Problem with Surface │
│ Temperature or Heat Transfer Coefficient Boundary│
│                  Condition                    │
└─────────────────────────────────────────────┘
                       │
                       ▼
┌─────────────────────────────────────────────┐
│      Run ANSYS, Obtain Transient Temperature  │
│                  Distribution                 │
└─────────────────────────────────────────────┘
                       │
                       ▼
┌─────────────────────────────────────────────┐
│   Run CONTRA with Transient Temperature Distribution │
└─────────────────────────────────────────────┘
                       │
                       ▼
┌─────────────────────────────────────────────┐
│   CONTRA Calculates the Transient Heat Transfer │
│       Coefficient and Surface Temperature     │
└─────────────────────────────────────────────┘
                       │
                       ▼
┌─────────────────────────────────────────────┐
│        Compare CONTRA and ANSYS Results       │
└─────────────────────────────────────────────┘
```

Figure 440.361-1 Validation of CONTRA Using ANSYS Calculations

Westinghouse

AP600
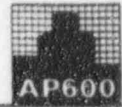
Case 1 Results for ANSYS Run PIPE1

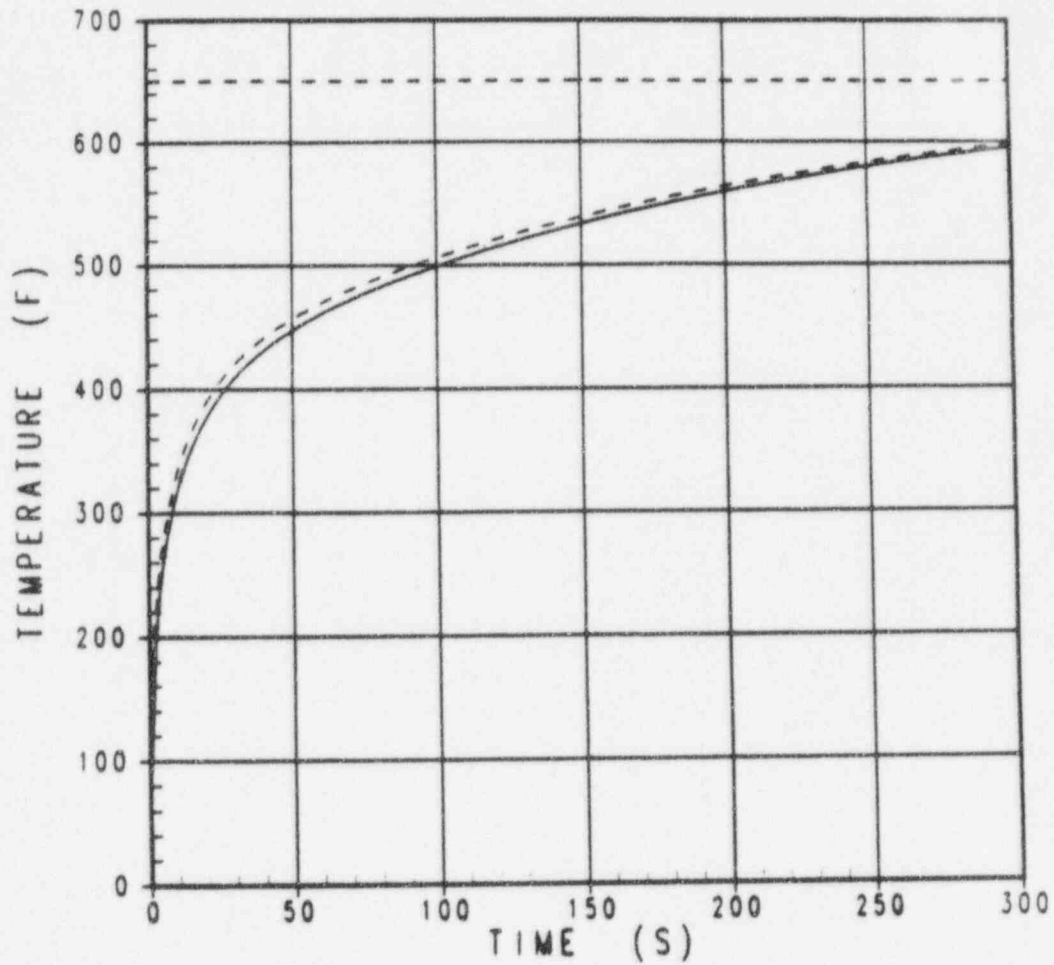| | | | | |
|---|---|---|---|---|
| —— T2 | 1 | 20 | 1 | T METAL 1 |
| – – – T-WALL | 1 | 20 | 1 | SURFACE TEMPERATURE |
| – – – TFL | 1 | 20 | 1 | T FLUID |

Figure 440.361-2

AP600

Case 1 Results for ANSYS Run PIPE1
——— Calculated Surface Temp. Error: T-Wall – T1



Figure 440.361-3

Westinghouse

AP600

Case 1 Results for ANSYS Run PIPE1
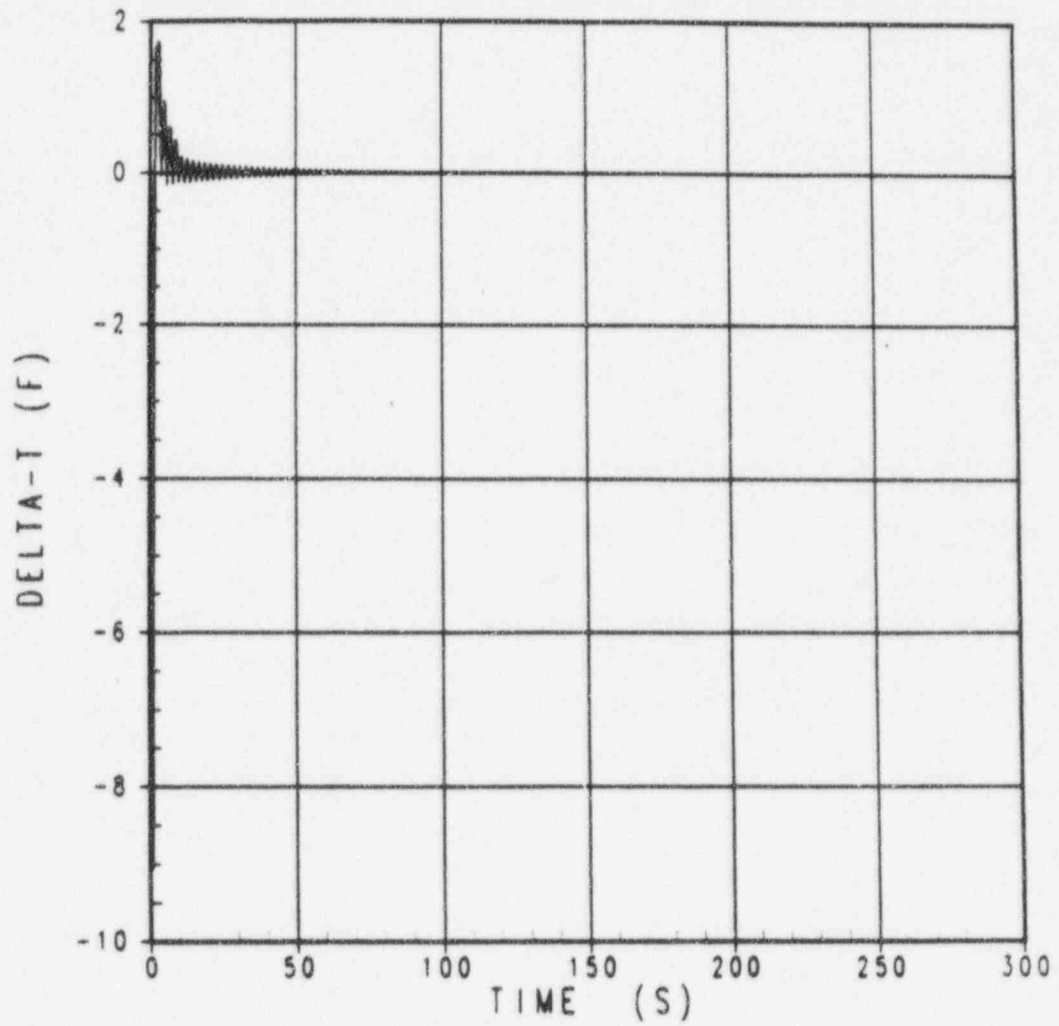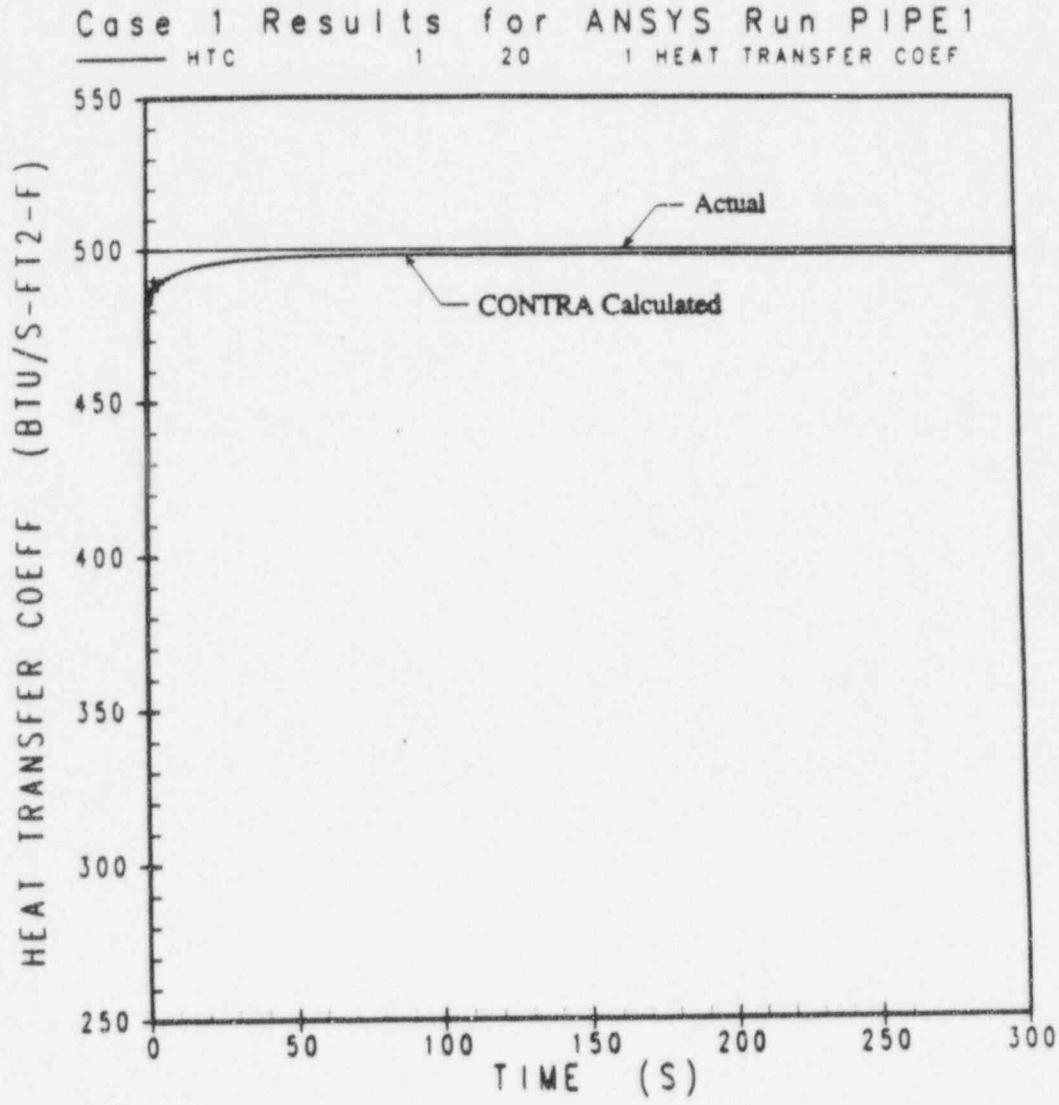HTC          1    20     1 HEAT TRANSFER COEF



Figure 440.361-4

AP600

Question 440.362

Re: CMT Final Data Report and Final Test Analysis Report

A conventional definition of film condensation heat transfer coefficient, h, is the thermal conductivity of the liquid (k) in the film divided by the film thickness δ, or

$$h = k/\delta$$

while in the TAR, an alternative definition is used based on heat flux and an estimated temperature difference. When one examines the behavior of the condensation heat transfer coefficient, it does not, in many cases, seem to follow the trends one would expect in either the laminar or turbulent regimes (for example, see TAR Figure 4.2-12). The unconventional approach used in determining h may be partly responsible for the behavior shown for these parameters. Provide a justification for the approach used, and explain how the apparent uncertainty in determining condensation heat transfer might potentially affect the calculated behavior of the CMT.

Response:

The laminar condensation heat transfer coefficient is defined as the conduction resistance across the condensate film as indicated in the RAI. However, in the CMT experiments, the condensate film could not be measured so this approach was not be used. Instead, the metal temperatures were measured within the CMT tank wall and were used with an inverse conduction technique to calculate the heat flux at the inner CMT surface. This heat flux was then divided by the extrapolated CMT wall temperature-to fluid-temperature difference to obtain a local heat transfer coefficient. The inverse conduction approach is a standard technique used to obtain wall heat fluxes and heat transfer coefficients from experimental data. This approach has been used successfully in the PWR FLECHT and FLECHT-SEASET programs for calculating reflood heat transfer coefficients (see References 440.362-1 and 440.362-2).

The potential errors in using the inverse conduction technique for the CMT tests are the representation of the temperature gradient close to the inside surface of the CMT tank, the location of the thermocouples in the wall, the contact of the thermocouples with the wall, and the properties of the wall, all of which were used in the calculation. Thermocouples were specifically placed at and near the inside surface to measure the gradient in this area as accurately as possible. A detailed one-dimensional numerical analysis model of the CMT tank wall was used to help place the thermocouples. Also as described in the CMT Facility Description Report (Reference 440.362-3), care was used in peening the thermocouples into the holes in the CMT walls using a copper washer to insure good thermal contact. The hole depth was accurately measured for each thermocouple during installation such that the correct location of the measurement was known for the inverse conduction analysis. In addition, a sample of the CMT steel was analyzed to obtain its thermal-physical properties such that the heat flux calculation would be accurate. If the temperature gradient is underestimated from the CONTRA fit to the measured temperatures, and the measured temperatures smooth the sharp radial temperature profile within the CMT wall, the heat flux calculated form the CONTRA calculation may be initially be underestimated. As time progresses, and the temperature profile becomes established in the wall, the calculation becomes more accurate.

W Westinghouse

AP600

Therefore, the areas where uncertainty could effect the resulting heat transfer coefficient calculation from an inverse conduction method were addressed in the experiment such that the most accurate values would be calculated form the data.

References

440.362-1    Rosal, R. et. al., "FLECHT Low Flooding Rate Cosine Series Tests," WCAP-8651, December 1975

440.362-2    Loftus, M. J., et. al., "PWR FLECHT-SEASET Unblocked Bundle Forced and Gravity Reflood Task; Data Report," WCAP-9699, June, 1980

SSAR Revision:  NONE

Westinghouse

Question 440.440

Re: NOTRUMP CMT PVR (MT01-GSR-011)

Thermal stratification in the CMTs is a major modeling concern in the AP600 simulations. On page 4-2, comparisons of the NOTRUMP code to test data, demonstrate that the code tendency is to overpredict the temperatures in the CMT and as a consequence overpredicts the drain flow rates. As such, was a nodalization study performed to justify the use of four nodes in the CMT? Fig. 2-5 shows a much larger lower node was used at the bottom of the CMT, please explain why this nodalization was used. The poor comparisons with temperature suggest more nodes are required. More nodes may not eliminate the numerical diffusion, but the errors in the NOTRUMP temperature prediction should be reduced with additional nodal detail in the CMT. Please provide the results and discussion of the nodalization study used to justify this spacial model. Also, provide plots of the fluid driving heads calculated by NOTRUMP for each side of the loop shown in the system model in Fig. 3-1. These plots should help to understand the inlet and outlet flow behavior in NOTRUMP for the tests.

Response:

The thermal stratification effects in the CMT are not identified as a specific thermal-hydraulic phenomena on the final small-break LOCA PIRT chart, given as Table 4 in the response to RAI 440.325. However, the CMT recirculation effects are ranked important and the temperature distribution within the CMT does have an effect on the driving head for the recirculation flow. The NOTRUMP comparisons to the average of the fluid temperature data indicate very good agreement for the top fluid node in the NOTRUMP CMT model as seen in Figures 4.2-4, 4.2-13, 4.3-4, 4.3-13, and not as good agreement as indicated in Figure 4.2-22 from Reference 440.440-1. The lower nodes in the CMT model indicate an earlier diffusion of the hot CMT liquid into the lower nodes and a resulting lower maximum temperature for those nodes, when compared to the average of the test data.

There is also thermal diffusion effects in the reservoir volume since this is modeled as a single fluid node. The effects of this reservoir thermal diffusion is apparent at later times in the transient when NOTRUMP predicted temperatures decrease relative to the data.

The NOTRUMP CMT noding has 10 % of the CMT volume in the top node, including the entrance nozzle, 15 % of the volume in each of the next two nodes and 60 % in the bottom most node. The basis for the selection of these volumes was a noding sensitivity study which was performed when analyzing the 300 series CMT tests (Reference 440.440-2). The 300 series examined the condensation and mixing of the balance line steam with the colder CMT liquid. The parameter which was of interest was the delay time of the CMT drain flow which was reduced because of the condensation at the top of the CMT. The use of the four nodes with the volumes given above gave the best results when compared to CMT drain delay times for the variation in noding which was examined. Another basis for the selection of the size of the first node is that its volume includes the volume which would be directly influenced by the diffuser in the CMT entrance nozzle. The purpose of the diffuser in the entrance nozzle of the CMT is to limit the mixing of the hot recirculated water or the balance line steam such that a stable hot liquid layer is quickly formed. This behavior of the diffuser was confirmed by the tests. Therefore, the noding for the lower portions of the CMT could be coarse since the mixing effects occurred at the top of the CMT.

The technical issue is that any code like NOTRUMP or RELAP will have a difficult time modeling a moving thermal front such as that observed in the CMT 500 series tests during the CMT recirculation phase. Numerical diffusion

AP600

will occur as the hot liquid from one cell flows into and mixes with the cell below it at a given time. As the RAI indicates, additional nodes will not eliminate the numerical diffusion, but may provide a more accurate simulation of the axial temperature gradient in the CMT. However, it is not clear that the additional complexity of increased noding will yield improved response for simulating the CMT behavior.

Using the noding as given in Reference 440.440-1, the agreement between the average measured drain flow and the predictions is quite good as seen in Figure 5-1 of Reference 440.440-1. Also, the same noding was used for the OSU and the SPES integral simulations as was used in the CMT tests. The comparisons of the CMT drain flows during the recirculation period on up to approximately 500 seconds in the SPES tests ( Reference 440.440-3) was very good as seen in Figures 5.1-15 and 5.1-16 of Reference 440.440-3 for Test S00303. The comparisons were not as good in Figure 5.2-15, but were much better in Figure 5.2-16 for Test S00605 for the first 400 seconds. The poorer agreement in Figure 5.2-15 does not affect the overall CMT performance since, the CMT empties at about the same time as the data. The comparisons for Test S00708, shown in Figure 5.3-15 of Reference 440.440-3 is also reasonably good.

Similar comparisons have been made during the CMT recirculation period in the OSU Preliminary Validation report, Reference 440.440-4, for test SB01 in Figures 5.1-15 and 5.1-16 for approximately the first 200 seconds. The comparisons are not as good in Test SB10, but the recirculation period is much shorter for this test since it is a much larger break (approximately 50 seconds). The CMT recirculation flow comparisons for test SB14 are shown in Figures 5.5-15 and 5.5-16 and show reasonably good agreement for the 70 second recirculation period.

The noding that has been used in NOTRUMP for the CMT does give good agreement with the CMT separate effects tests and the SPES and OSU integral systems tests for the CMT recirculation behavior which is highly ranked in the PIRT.

The 500-series CMT tests will be reanalyzed in the NOTRUMP Final V&V report. When these tests are reanalyzed, the CMT will be simulated with flow and enthalpy boundary conditions such that the additional numercial diffusion caused by the steam/water reservoir will not be present. As part of the comparisons, the driving heads calculated by NOTRUMP will be provided with the reanalyzed cases.

References

440.440-1   Jaroszewicz, J. and L. E. Hochreiter, "AP600 NOTRUMP Core Makeup Tank Preliminary Validation Report for 500-Series Natural Circulation Tests" , MT01-GSR-011, april 1995.

440.440-2   Cunningham, J.C., et.al. "AP600 NOTRUMP Core Makeup Tank Preliminary Validation Report", MT 01-GSR-001, October, 1994.

440.440-3   Meyer, P.E. et al, "Notrump Preliminary validation Report for SPES-2 Tests", PXS-GRS-002, July, 1995.

440.440-4   Willis, M. G. et al. "NOTRUMP Preliminary validation report for OSU Tests" LTCT-GRS-001, July,1995.

440.440-2                                                                                                  (W) Westinghouse

AP600

SSAR Revision: NONE

AP600

Question 440.464

Re: NOTRUMP PVR FOR OSU TESTS, LTCT-GSR-001, JULY 1995

440.464  The core region is modeled as four volumes, yet there is no justification for this choice in nodalization. This simplified nodalization may not produce the correct void distribution in the core and will result in an over prediction of the two-phase level in the vessel core and upper plenum.  Thus, the potential for this over-simplified core model to predict the potential for core uncovery is minimized or precluded.  Please show that the core nodalization captures the correct void distribution in the core and the resulting two-phase level in the vessel characteristic of small break LOCAs in AP600.  Please provide justification that this model/nodalization will properly capture the potential for core uncovery following small breaks.  Provide comparisons to transient two-phase level swell and  test bundle uncovery data in separate effects tests to justify the model/nodalization (Please see RAI 440.515 below for candidate separate effects tests).  The comparisons of NOTRUMP to the four steady-state THTF tests in "Westinghouse Small Break ECCS Evaluation Model Using the NOTRUMP Code," WCAP 10054-P-A, dated August 1984, is not sufficient to demonstrate the ability of the NOTRUMP code to accommodate transient two-phase level swell phenomena.  Please describe how the code computes steam release from the two-phase surface in the vessel.

Response:

As noted in response to RAI 440.515, Westinghouse will perform analysis of the G-2 level swell experiments given in EPRI report EPRI-NP-1692.  This information will supplement that for the THTF tests contained in reference 440.464-1 which would be sufficient to demonstrate the core noding if there were no coding changes.  For the G-2 level swell experiments, tests will be simulated over the full pressure range given in the test data at different bundle powers.  Comparisons of the mixture height and void distribution as a function of time will be provided to justify the choice of core nodalization.

The computation of steam release (bubble rise) from the two-phase surface of a stratified fluid node is described in the response to RAI 440.474.  It should be noted that the nodes representing the lower plenum, core region, and upper plenum are all part of a common stack (see the response to RAI 440.483).  Thus, at any given time, only one node of the stack has two regions with bubble rise and droplet fall between the regions.  Phase separation between all nodes in the stack is accomplished by drift flux in the links connecting the stacked nodes.


References

440.464-1    N. Lee, et. al., "Westinghouse Small Break ECCS Evaluation Model Using the NOTRUMP Code," WCAP-10054-P-A (Proprietary), WCAP-10081-P (Non-proprietary) August 1985.

SSAR Revision:  NONE

---

(W) Westinghouse

Question 440.493

Re: NOTRUMP PVR FOR OSU TESTS, LTCT-GSR-001, JULY 1995

440.493 Please explain why the NOTRUMP code depressurizes much faster than the data in Fig. 5.3-1. What break flow discharge coefficients were used for this simulation. Discuss the influence of the steam generator heat transfer model on the pressure transient early in the event. Also, explain why and justify that the faster depress. zation will not lead to non-conservative predictions of AP600 plant and ECC performance.

Response:

Examination of the NOTRUMP predictions indicate that the flow rate through the broken balance line on the cold leg is higher than the test data. As a result, NOTRUMP predicts drainage of the pressurizer early, after only 11 seconds compared with 45 seconds in the test. The earlier draining of the pressurizer in NOTRUMP causes the earlier decrease in system pressure, but subsequent rate at which the pressure decreases agrees well with the data. The difference in pressure is maintained throughout the first 400 seconds and disappears following initiation of ADS stage 2 in the test at 300 seconds. A break flow multimplier of unity was used in the NOTRUMP simulation. In NOTRUMP the sub-cooled break flow rate is given by Henry-Fauske correlation, which transitions to the homogenous equilibrium model as flow quality increases. The NOTRUMP steam generator secondary mixture temperature prediction indicates that no significant heat transfer from the primary to secondary takes place in the first 50 seconds of the simulation, refer the Reference 440.493-1.

In terms of primary mass inventory, the higher drain rate predicted by NOTRUMP brings forward in time the prediction of minimum core inventory and minimum sub-cooled level (see Reference 440.493-2), thereby increasing the corresponding decay heat level, which is conservative.

References

440.493-1   Response to RAI 440.512, November, 1995

440.493-2   Response to RAI 440.492, December, 1995

SSAR Revision: NONE

Question 440.509

Re: NOTRUMP PVR FOR OSU TESTS, LTCT-GSR-001, JULY 1995

440.509  Please explain why the NOTRUMP code overpredicts the ADS flow rates in Figs. 5.5-18 and 5.5-19 in view of the fact that system pressure is well predicted during this time period.

Response:

Following the initiation of ADS stage 4 the flow through ADS stages 1-2-3 is terminated in the test. At this time the DVI flow, which is basically IRWST injection, is balanced by the flow through the ADS stage 4 valves. The NOTRUMP simulation differs from the test data in that the flow through ADS stages 1-2-3 terminates earlier, so that the integrated mass lost is approximately 500 lbm less than the test data at the initiation of ADS stage 4, which occurs slightly later in the NOTRUMP simulation compared to the test data. Since NOTRUMP initially predicts higher injection flow rates from the IRWST compared to the test data (discussed in Reference 440.509-1), the ADS stage 4 flow rates are also higher compared to the test data to reach a quasi-equilibrium.

References

440.509-1   Response to RAI 440.514, November, 1995

SSAR Revision:  NONE